

1 Morphological aspects of immature stages of *Migonemyia migonei* (Diptera:  
2 Psychodidae, Phlebotominae) an important vector of Leishmaniosis in South America  
3 by scanning electron microscopy

4  
5 Eric F. Marialva<sup>1,3\*</sup>, Nágila F. Secundino<sup>2</sup>, Fernando F. Fernandes<sup>2,4</sup>, Helena R. C.  
6 Araújo<sup>5</sup>, Claudia M. Ríos-Velásquez<sup>1</sup>, Paulo F. P. Pimenta<sup>2</sup>, Felipe A. C. Pessoa<sup>1</sup>

7  
8 <sup>1</sup> Laboratório de Ecologia de Doenças Transmissíveis na Amazônia, Instituto Leônidas  
9 & Maria Deane - Fiocruz Amazônia, Manaus, Amazonas, Brazil

10 <sup>2</sup> Laboratório de Entomologia Médica, Instituto René Rachou - Fiocruz Minas Gerais,  
11 Belo Horizonte, Minas Gerais, Brazil

12 <sup>3</sup> Programa de Pós Graduação em Biologia da Interação Patógeno Hospedeiro, Instituto  
13 Leônidas & Maria Deane - Fiocruz Amazônia, Manaus, Amazonas, Brazil

14 <sup>4</sup> Division of Entomology, Federal University of Goiás, Goiânia, Goiás, Brazil.

15 <sup>5</sup> Instituto de Ciências Biomédicas, Departamento de Parasitologia, Universidade de São  
16 Paulo, São Paulo, Brazil

17

18 \* ericmarialva304@gmail.com

19

20

21

22

23

24

25

## 26 **Introduction**

27           In the last few decades, new proposals in phylogeny sand flies, especially based  
28 on adult morphology has been highlighted and several authors have adopted the Galati  
29 [1,2] proposal, that changed the taxonomy, phylogeny and nomenclature basis of  
30 phlebotomine systematic. However, the knowledge about several aspects of the  
31 immature stages of phlebotomine sand flies (Diptera: Psychodidae) is still a challenge,  
32 due to the difficulties of finding a natural breeding site or lab colonization. So, of about  
33 more than 537 species described in the Neotropics [1–3], larval stages or mature larvae  
34 and rarely pupae of only 92 species of the New World sand flies have been described, or  
35 partially described.

36           Larval structures are important for providing some highlights on taxonomy,  
37 phylogeny, and evolution of this subfamily. In the last few decades, new proposals have  
38 been highlighted on phylogeny of sand flies, especially based on adult morphology, and  
39 several authors have adopted the Galati proposal [1,2], which has changed the  
40 taxonomy, phylogeny and nomenclature basis of phlebotomine systematic.

41           The analysis of the microstructure of the immature stages of Phlebotominae, in  
42 addition to contributing to the discovery of other morphological characters capable of  
43 promoting taxonomic and phylogenetic studies, in order to better elucidate the evolution  
44 of this subfamily, also makes it possible to investigate the existence of sense structures  
45 used in the communication of these vectors, aiming at the development of alternative  
46 eco-friendly control strategies.

47           The use of scanning electron microscopy (SEM) has significant improved the  
48 characterization and descriptions of immature forms, and provided details of larval  
49 chaetotaxy [4,5]; ontogeny [6–8]; spiracles [9,10]; antennal, and mouthparts, such as the  
50 sensilla as well as caudal bristles [7,11,12]. Despite this, only a few articles have been

51 carried out about the pupal morphology of New World phlebotomine sand flies [8,13–  
52 16]. Therefore, the number of descriptions of immature forms of sand flies still remains  
53 scarce.

54 The sand fly, *Mg. migonei* (França), is an important vector of *Leishmania*  
55 (*Viannia*) *braziliensis*, and one of the causative agents of cutaneous leishmaniosis in  
56 South America, especially in Brazil [17–19]. Torrellas [20] found *Mg. migonei* infected  
57 with *Le. guyanensis* and *Le. mexicana* in an Andean region of Venezuela. Studies  
58 confirmed that this species is also associated with the transmission of *Leishmania*  
59 *infantum chagasi* in Brazil and Argentina [21,22].

60 Despite the importance of its immature morphology, few studies have been  
61 carried out, especially under scanning electron microscopy (SEM). These were  
62 restricted to the description of the larvae antennae [11] and spiracles [9,10] and to the  
63 egg exochorion [23,24].

64 The present study aims to provide a complete morphological analysis of the  
65 surface of immature stages of *Mg. migonei*, in order to reveal taxonomic characters that  
66 can support future works on phylogenetics and systematics involving immature stages  
67 of this vector.

## 68 **Material and Methods**

69 The eggs, larvae and pupae of *Mg. migonei* were acquired from a stable colony  
70 maintained in laboratory conditions, whose parents were obtained in the municipality of  
71 Baturité, Ceará state, Brazil. The species was bred at the laboratory facilities of  
72 Leônidas & Maria Deane Institute, Manaus, Amazonas state, according to the method  
73 described by Lawyer [25]. Some of the larvae from each larval instar (1<sup>st</sup> to 4<sup>th</sup>) and  
74 pupae were slide-mounted in Berlese fluid. Measurements of the body's bristles were  
75 made under eye pierce using light microscopy.

76 Morphology and chaetotaxy of the head were observed following the  
77 methodology of Arrivillaga[26], which indicates the morphology and setae of the  
78 mouthparts with taxonomical importance. Chaetotaxy of the body followed the system  
79 used by Ward [27]. The chaetotaxy of the pupae used in this study followed the  
80 terminology proposed by Oca-Aguilar [8]. Systematic classification follows that  
81 proposed by Galati [2], and abbreviations of the genera follow Marcondes [28]. In  
82 addition, both species were studied and photographed under scanning electron  
83 microscopy. Some reared larvae were killed in hot water (70°C), fixed in 3%  
84 glutaraldehyde and then washed thoroughly in phosphate-buffered saline; and the  
85 solution was changed every 30 min over a period of six hours. Subsequently, they were  
86 fixed in osmium tetroxide, dehydrated in a series of ethyl alcohol concentrations,  
87 submitted to critical point drying in carbon dioxide and sputtered with 25 MA colloidal  
88 gold [7,11]. The specimens were examined in a scanning electron microscope  
89 (JSM5600, JEOL, Tokyo, Japan) at an accelerating voltage of 7 KV and then  
90 photographed. Tables were mounted showing the differences in chaetotaxy between the  
91 instars of each species and between species.

## 92 **Results**

93 **Egg of *Mg. migonei*:** The egg is elongated, with one side slightly flattened,  
94 measuring 323 (300-351)  $\mu\text{m}$  in length and 94.8 (89-107)  $\mu\text{m}$  in width (N=4) (Fig.1A). The  
95 exochorion is formed by a thin basal lamina that supports their ornaments or sculptures with  
96 polygonal reticulation, which comprises ridges, usually continuous, forming alternating  
97 transversal rows of generally rectangular parallel cells or square to polygonal cells (Fig. 1B).

98

99 **Fig 1. Scanning electron microscopy of the eggs of *Migonemyia migonei*.** A, general view of the egg  
100 showing an ornamentation characterized by the presence of ridges arranged in a polygonal pattern (rpp;  
101 scale bar: 50  $\mu\text{m}$ ); B, eggshell ornamentation showing detail of the ridges (Scale bar: 10  $\mu\text{m}$ ).

102

103           **General appearance of the larvae of *Mg. migonei*:** The larva is caterpillar-like,  
104 with a well-sclerotized hypognathous, non-retractile head with very short antennae with  
105 short basal tubercle. The dark brownish colour head and body tegument are covered by very  
106 small spines and tubercles in a scattered distribution. The thorax includes prothorax, with the  
107 anterior spiracle borne laterally, and other two segments (meso and metathorax). Its  
108 abdomen is nine-segmented, covered by brown pale setae and the body tegument is  
109 yellowish, with a pair of posterior spiracles borne laterally on a short tubercle.

110           Caudal filaments (or caudal setae), long sensilla of the trichoid type that exhibit many  
111 wall pores, implanted between non-parallel ridges and that interconnect (or which overlap),  
112 darkened, were observed double-paired in the last three instars, or simply paired when is in  
113 the first instar (Fig. 2A-B).

114           The head is dark brown (Fig. 2A, 3A), body colour is pale with darkened eighth and  
115 ninth abdominal segments and bears tiny spines in all segments (Fig. 2A, Fig 7), the first  
116 instar is present a prominent egg buster (Fig 3C-D) with peculiar shape. There are three  
117 types of setae, usually distributed in pairs: a barbed brush-like setae (of brush-like trichoid  
118 sensilla type), more widely distributed on the larval head and body (Fig.3A, seta 2) and, a  
119 little barbed (weakly brush-like trichoid sensilla; Fig. 3A, seta 1) and a simple, bare paired  
120 setae (trichoid sensilla; Fig. 3A, seta 6). The size and the type of setae are shown in Table 1.

121

122   **Fig. 2. Scanning electron microscopy of the fourth, and first instar larva of *Migonemyia migonei*.** A,  
123 observation of first (1st) and fourth (4th) instar larvae, besides of the number of body segments and  
124 caudal filaments (scale bar: 200µm); B, higher magnification of the surface of the caudal filament  
125 showing pores implanted between non-parallel, interconnected and overlapping ridges. (scale bar: 5µm).  
126 Caudal filaments (cf), head (h), protorax (pt), mesotorax (mst), metatorax (mtt), ridges (rdg), and pores  
127 (po).

128 **Head:** The head is capsule-like, broader than it is high. The tegument is covered by thin,  
129 small spicules of the microtrichia type. On the dorsal part of the head (Fig.3A), the cephalic  
130 tagma has the following setae: the anterior frontoclypeal setae (1 weakly brush-like trichoid  
131 sensilla, subtype) with spinulate form, the posterior frontoclypeal setae (2; brush-like trichoid  
132 sensilla, subtype) with barbed shape, the anterior genal setae (3) with a simple spine form.  
133 The medial genal (4) and posterior genal (5) setae are barbed brush-like (brush-like trichoid  
134 sensilla, subtype). In the ventral part (Fig. 3B), the postgenal (6) and subgenal (7) are simple  
135 setae (Table 1). All setae are inserted in small tubercles. In the first instar larvae, the setae 1  
136 is usually simple; however, it is possible to predict the projection of those setae becoming  
137 barbed at the other subsequent instars. Each of the antennae of *Mg. migonei* larvae (Fig. 4A-  
138 B) has a basal tubercle (socket) that is a small and cylindrical segment fused at a second  
139 ovoid distal segment. This segment presents an antennal organ, which is equipped with a  
140 longitudinal furrow in the posterior surface, and is more evident in the 1<sup>st</sup> instar antennae, as  
141 well as three short structures in the base of the segment. The central structure is wider than it  
142 is long and shorter than the laterals ones (Figs. 4A-B). The apex of antennae exhibits a single  
143 apical clavate basiconic sensillum and, from a lateral groove, four sensilla of the *coeloconica*  
144 type emerge: three smaller with blunt apex – noting that the middle one (smaller coeloconic  
145 sensillum, subtype) is wider, shorter and less cylindrical than the two that are on the sides  
146 (blunt coeloconic sensilla, subtype) – and, between these three, behind, one larger and  
147 clavate (clavate coeloconic sensillum, subtype; Figs. 4A-B).

148

149

150 **Fig 3. Scanning electron microscopy of the larva of *Migonemyia migonei*.** A, Head of the fourth instar  
151 larval in dorsal and ventral view B. Long trichoid sensilla observed at the apex of the head (lts) and the  
152 short trichoid sensilla on the mouthparts (arrows; A and B scale bars: 20 µm); C, Head in dorsal of the  
153 first. On the forehead are two weakly brush-like trichoid sensilla (wb-lts) inserted slightly forward and

154 between the antennae (ant) and long trichoid sensilla (lts) are inserted furtherdown toward the mouthparts  
 155 (scale bar: 20  $\mu$ m). D, Egg buster (eb). cl, clipeo; md, mandible; ma, maxilla; m, mentum. The setae were  
 156 numbered according to the chaetotaxy proposed in study: (1 = wb-lts) frontoclipeal anterior setae (weakly  
 157 brush-like trichoid sensilla); (2 = b-lts) frontoclipeal posterior setae with barbed shape (brush-like trichoid  
 158 sensilla); (3 = lts) the genal anterior setae with a simple spine form (long and bare trichoid sensilla); the  
 159 genal medial (4) and genal posterior (5) are barbed brush-like setae (= brush-like trichoid sensilla). In the  
 160 ventral part (Fig. 3B), the postgenal (6) and subgenal (7) are simple setae (bare trichoid sensilla)

161

162 **Fig 4. Scanning Electron Microscopy of the larva of *Migonemyia migonei*.** A, antenna of the first  
 163 instar larva (scale bar: 5  $\mu$ m); B, antenna of the fourth instar larva (scale bar: 10  $\mu$ m). It is observed in A  
 164 and B, a single apical clavate basiconic sensillum (acbs) at the apex of the antennae and, emerging from a  
 165 lateral groove, one smaller coeloconic sensillum (scs) and two blunt coeloconic sensilla (bcs) and,  
 166 between these two, behind, one clavate coeloconic sensillum (ccs).

167

168

169 **Table 1. Corresponding numbers and size of the setae of each segment (size in  $\mu$ m,**  
 170 **N=4) of fourth to first instar larvae of *Migonemyia migonei*.**

Larva body part	<i>Migonemyia migonei</i>					
	Setae number	Type of setae	Size of the setae in the corresponding larval instar			
Head		Bristle	4 <sup>th</sup>	3 <sup>rd</sup>	2 <sup>nd</sup>	1 <sup>st</sup>
Frontoclipeal anterior	1	Spinulate	93.3	77.4	65.4	52.0
Frontoclipeal posterior	2	Barbed	85.3	65.3	50.7	29.4
Genal anterior	3	Simple	113.0	70.65	60.0	41.4
Genal medial	4	Barbed	93.3	64	53.3	44.0
Genal posterior	5	Barbed	90.7	62.7	46.7	33.4
Postgenal	6	Simple	101.3	64.0	54.7	37.3
Subgenal	7	Simple	80.0	37.3	24.0	13.3

Prothorax						
Dorsal internal	1	Barbed	85.0	57.3	46.7	38.7
Dorsal intermediate	2	Barbed	65.0	41.35	20.0	24.0
Dorsal external	3	Barbed	87.5	60.0	49.4	NO
"Shoulder" accessory	a	Spine	25.0	17.4	17.7	NO
"Shoulder" accessory	b	Barbed	16.0	08.0	08.0	NO
Anterior ventrolateral	4	Barbed	100.0	61.3	45.4	32.0
Ventral external	5	Barbed	67.5	55.0	49.4	30.7
Ventral internal	6	Barbed	100.0	64	53.3	29.3
Dorsal submedian	7	Barbed	90.0	49.3	33.4	16.0
Mid-dorsal	8	Barbed	100.0	64.0	44.0	18.7
Dorsolateral	9	Barbed	95.0	52.0	40.0	26.7
Basal	10	Barbed	42.5	22.7	12.0	NO
Post-ventrolateral	11	Barbed	96.0	53.35	44.0	30.7
Post-ventral	12	Spine	13.3	6.7	6.7	6.7
Mid ventral	13	Barbed	72.0	42.6	26.7	12.0
Ventral intermediate	14	Barbed	17.3	12.0	NO	2.7
Ventral submedian	15	Barbed	38.7	21.35	13.3	8.0
Meso and metathorax						
"Shoulder" accessory	a	Spine	14.7	10.7	8.0	6.7
"Shoulder" accessory	b	Barbed	17,3	9,35	8.0	NO
Anterior ventrolateral	4	Barbed	90.0	52.0	37.4	25.4
Dorsal submedian	7	Barbed	142.5	69.35	37.4	20.0
Mid-dorsal	8	Barbed	152.5	78.65	46.7	21.4
Dorsolateral	9	Barbed	127.5	65.3	42.7	29.3
Basal	10	Barbed	25.0	13.3	8.0	NO
Post-ventrolateral	11	Barbed	78.8	49.3	36.0	17.4
Post-ventral	12	Spine	14.7	9.35	NO	05.3
Mid-ventral	13	Barbed	77.3	38.65	29.3	14.7



Ventral intermediate	14	Barbed	22.7	13.3	8.0	4.0
Ventral submedian	15	Barbed	44.0	21.4	14.7	9.4
Abdominal segments 1–7						
Dorsal intermediate	2	Barbed	35.0	12.0	5.33	2.7
Anterior ventrolateral	4	Barbed	102.5	48.0	34.65	16.0
Dorsal submedian	7	Barbed	165.0	76.0	38.70	17.4
Mid-dorsal	8	Barbed	180.0	93.3	50.65	20.0
Dorsolateral	9	Barbed	165.0	82.65	48.0	41.4
Post-ventrolateral	11	Barbed	75.0	44.0	36.0	18.7
Post-ventral	12	Barbed	30.0	13.3	10.7	NO
Ventral submedian	15	Simple	66.7	37.3	32.0	17.4
“C”-		Spine	12.0	9.35	8.00	NO
Abdominal segment 8						
Anterior ventrolateral	4	Barbed	77.3	34.7	25.4	NO
Dorsal submedian	7	Barbed	46.7	20.0	10.7	10.7
Mid-dorsal	8	Barbed	147.15	88.0	57.3	12.0
Dorsolateral	9	Barbed	118.8	69.4	45.3	37.3
Post-ventrolateral	11	Spinulate	52.0	28.0	25.4	12.0
Post-ventral	12	Spine	22.0	12.0	6.7	8.0
Ventral submedian	15	Spinulate	57.3	26.7	25.4	9.35
“Should accessory”	A	Spine	14.7	6.7	5.4	NO
“Should accessory”	B	Spine	29.3	12.0	9.4	5.3
Abdominal segment 9						
Anterior ventrolateral	4	Simple	220	152	137.5	92.0
Dorsal submedian	7	Simple	95.9	64.0	46.7	34.7
Mid-dorsal	8	Barbed	57.3	33.4	24.0	52.0
Dorsolateral	9	Barbed	57.3	36.0	24.0	16.0
Post-ventrolateral	11	Simple	97.2	48.0	38.7	21.3
Post-ventral	12	Simple	48.0	22.7	21.3	9.35

Ventral submedian	15	Simple	37.3	21.3	14.7	13.3
Internal caudal	IC	Simple	1250	950	720	560
External caudal	EC	Simple	1045	625	565	NO

171 NO: Not observed

172 Mouthparts: The external part of the mouth is composed of a pair of mandibles,  
173 a pair of maxillae, labrum, and mentum. Each segmented mandible bears two simple  
174 setae in the middle of the dorsal part (S1 and S2), and a simple seta (S6) in the superior  
175 margin of the mandible, which are similar to those described by Pessoa et al. (2008). In  
176 the lower part of the mandible, there are five strong teeth, a proximal (T3) nearest the  
177 molar lobe (ML), an apical single (T1), and double-paired median tooth (T2 - that are  
178 observed, in light microscope, as a single tooth) (Fig. 6).

179 Each maxilla has three simple setae, an S1 in the apical dorsal part, and two (S2  
180 and S3) in the proximal part (Fig. 5). There is a maxillary process in the middle of this  
181 structure. In the margin of the dorsal part, there is a sequence of a small and sparse  
182 comb of spines, similar to those found in the maxilla of *Ev. lenti* and *Ev. carmelinoi*  
183 [12]. At the apex, there are papilliform and trichodea sensillae (spinous hairs). On the  
184 upper side, there is a row of small setae. The ventral surface of the labrum is covered  
185 with parallel, transverse rows of finger-like combs of setae; the dorsal side has two pairs  
186 of very small simple setae. The clypeus has two pairs of simple setae, the distal pair is  
187 small, and the apical bigger (Fig. 5).

188 **Fig 5. Scanning electron microscopy of the mouthparts of fourth instar larva of *Migonemyia***  
189 ***migonei***. L, labrum; md, mandible; mx, maxila; me, mentum; s1-s6, mandible setae; s1\*-s3\*, mx : maxila  
190 setae; maxillary palpus (scale bar: 20 µm).

191

192

193 **Fig 6. Mandible of *Migonemyia. migonei* larva.** Apical (T1), double paired median tooth (T2),  
194 proximal (T3) and molar lobe (ml). Proximally, setae of the trichoid sensilla type (S1 and S2) are  
195 observed and, below these, a small seta (arrow) and, under the margin, the ends of three other setae  
196 (arrowhead; scale bar:10  $\mu$ m).

197 .-

198

199 The thorax has three segments, the prothorax has the appearance of two segments,  
200 and the meso and metathorax are homologous with the posterior setae of the prothorax.  
201 Chaetotaxy follows the same pattern of setae as classified by Ward [27] and is presented in  
202 Table 1, and Figures 7 and 8. The anterior spiracles are conical and have eight to nine  
203 papillae (Fig. 9A), though five to six in the third instar larvae, and 4 in the second instar  
204 larva (Fig. 9B). However, we did not obtain clear images of the first instar larva in order to  
205 compare or count.

206 **Chaetotaxy of prothorax:** The tergite has two rows of setae. The first row has three  
207 pairs of setae: the dorsal internal, dorsal intermediate and dorsal external, and the second row  
208 has two setae, which are the dorsal submedian and the mid-dorsal. The pleura has two setae,  
209 the anterior ventrolateral and the dorsolateral, which appear to change position in the larvae.  
210 These setae are similar, barbed or brushed-like and have only small differences in size (Table  
211 1). There is a spine hyaline seta, between the first and second rows of setae, usually near the  
212 ventrolateral setae. The sternite also has two rows of setae. The first with two similar pairs of  
213 setae, a little less barbed than the dorsal setae, the ventral external and the ventral internal.  
214 The second row has seven pairs of setae, including the seta b, with different size and shape  
215 (Table 1). They are the basal, post-ventrolateral, post-ventral, mid ventral, ventral  
216 intermediate, ventral submedian, and b setae. The meso and metathorax do not have the first

217 row of setae that those in the prothorax tergite and sternite have, and the setae are the same  
218 as of the second row of setae in the prothorax.

219

220

221 **Fig7. Scanning electron microscopy of the ventral part of abdomen and pseudopoda of**  
222 ***Migonemyia migonei*.** A-C, mature larvae; D, first instar larvae. asc: accessory setae, pd: pseudopod, \*  
223 ampliation accessory setae. (scale bars: 100  $\mu\text{m}$ , 20  $\mu\text{m}$ , 10  $\mu\text{m}$  and 10  $\mu\text{m}$ , respectively).

224

225

226 **Fig 8. Scanning Electron Microscopy of the mature larva of *Migonemyia migonei*.** A, Prothorax and  
227 Mesothorax in dorsal of the fourth instar larva; B, a - accessory setae C, - dorsal and ventral view. (scale  
228 bars: 50 and 100  $\mu\text{m}$ , respectively).

229

230

231 The setae of the abdomen have the same distribution that is proposed by Ward[27],  
232 with an absence of the setae number ten in each segment. The segments one to seven are  
233 homologous, with similar size and shape. In the anterior part of the pseudopodium, there is a  
234 simple pair of seta, which have a similar size to setae eleven and twelve, and these are not  
235 considered by other authors as a seta without taxonomic value. This seta is called "c" here  
236 (Table 1 and Fig.8C). The eighth and ninth segments are darker. The posterior spiracles are  
237 conical, with ten papillae. The shape and measurements of the setae are in Fig. 8A-B and  
238 Table 1. Chaetotaxy of the abdominal segments one to seven is as follows: In the tergite, the  
239 pairs of setae are not grouped, anterior dorsal intermediate is much smaller than the others,  
240 and the anterior ventrolateral is in the border with the pleura, and a row of pairs of setae on  
241 the dorsal submedian, mid-dorsal and dorsolateral, also in the border of the pleura. All of  
242 them are barbed and have different sizes (Table 1). The sternites (Fig. 8) have large

243 pseudopodia, with a few simple setae, the post-ventrolateral and the post-ventral are both  
244 very small, simple setae and a simple and large ventral submedian setae. In the anterior part  
245 of the pseudopodia, there is a pair of setae, which is very similar to the post-ventrolateral and  
246 the post-ventral, named the setae "c". The abdominal segments eight and nine lack  
247 pseudopodia. Abdominal segment nine ends in two tubercles, each of which bears a caudal  
248 filament (Fig. 8A). These tubercles, in the ventral side, also possess a large campaniform  
249 sensilla (Fig. 9B). The posterior spiracle has 14-11 papillae.

250

251

252

253 **Fig 9. Scanning electron microscopy of the fourth instar larva of *Migonemyia migonei*.** A, abdominal  
254 7-9 and in dorsal of the fourth instar; B, and ventral view. Setae numbered according to the chaetotaxy  
255 proposed in study; ps - posterior spiracle, \*increased area of a campaniform sensilla. Intermediate dorsal  
256 (2), Anterior ventrolateral (4), Submedian dorsal (7), Mid-dorsal (8), Dorsolateral (9), Post-ventrolateral  
257 (11), Post-ventral (12), Submedian ventral (15). Scale bars: 50  $\mu\text{m}$  and 100  $\mu\text{m}$ , respectively.

258

259

260 **Fig. 10. Scanning electron microscopy of the larvae of *Migonemyia. migonei*.** A, anterior spiracles of  
261 the third instar larva (scale bar: 5  $\mu\text{m}$ ); B, anterior spiracles (sp) of the second instar larva brush-like  
262 trichoid sensilla.

263

264 **Other larval instars:** The body sizes of the third to the first instar larvae are (from  
265 the head to the end of the ninth abdominal segment and with a maximum width at the  
266 metathorax) respectively: 1.7 and 0.27; 0.94 and 0.13; 0.56 and 0.09 mm. The first instar is  
267 easily identified by the presence of a unique pair of caudal setae (multiporous long trichoid

268 sensilla; Fig. 2B) and the absence of some bristles in the prothorax (seta 3, a, b and 10) and  
269 pro, meso and metathorax (b and 10) and the presence of the egg buster in the head (Fig.  
270 3D). The setae 6 and 14 of the prothorax are simple in this instar and barbed in the others.  
271 The setae 11 and 15 of the abdominal segment 8 are simple and, in the other instars, become  
272 almost barbed. Chaetotaxy for the other instars are the same of the fourth, but differ in size  
273 (Table 1). The pupa emerges from a Y shaped suture of the head of mature larva (Fig 11A-  
274 B).

275

276 **Fig. 11. Scanning electron microscopy pupae of *Migonemyia migonei*.** A-B emerging from a mature  
277 larva; st- suture opened from larva tagma head (scale bars of A and B: 500 and 100  $\mu$ m,  
278 respectively).

279

280

281

282 **Pupa description:** The pupa of *Mg. migonei* is claviform and divided by the  
283 cephalothorax and abdomen (Fig. 12A, 13, 15, 16). The pupa tegument has some small  
284 ornaments, such as small spines and setae, which are described in Table 3 and the body  
285 is covered by several small rounded tubercles. The pharate female pupa is longer (2.24  
286 mm, n = 5) than the pharate males pupa (2.05 mm, n = 5) (Fig. 17).

287 The cephalic sheath with antennal impressions shows outlines of all  
288 flagellomeres of the pre-imaginal stage. Mouth part sheath is smooth; clypeal sheath is  
289 conspicuous; sexual dimorphism presented in the maxillary sheath is shorter than the  
290 sheath of the labrum-epipharynx and hypopharynx in the males; head chaetotaxy  
291 with very small spines (Fig. 13) and are numbered (Table 3). Thorax with a large  
292 longitudinal crest in the middle of dorsal side, Y-shaped, the pro and mesothorax have a  
293 pair of prominent tubercles, the methatorax has two pairs, the latter is bigger than the

294 former (Fig. 12). There are also a pair of spiracles (ventilatory orifice per Oca-Aguilar  
295 et al., 2014) in the prothorax. The prothorax has 2 + 2 small setae in each one and a  
296 campaniform sensillae; mesothorax with 3 + 3 pairs of setae, one pair of them being  
297 long, chaotic, called prealar, not sharp at the tip, (length  $0.15 \pm 0.008$  mm,  $n = 5$ ) and  
298 are stout, originating from tubercles, and a large mesonotal tubercle with a continuous  
299 border (Fig. 12B); the mesonotal tubercle is considered here as part of the Y arm of the  
300 longitudinal crest, with scattered small rounded tubercles. Metathorax has four pairs of  
301 setae, some associated with tubercles, with a small bifurcation in the tip of each seta –  
302 1T and 3T (Fig. 12 D and F). Ventral side of the thorax has leg and wing sheaths, and a  
303 marked wing venation stamped into it, with row of rounded tubercles in each stamped  
304 venation (Figs. 12A, 15A and 16A).

305

306 The tegument of the abdomen is covered by several small, spiniform tubercles. There  
307 are nine segments, and the width of every segment is near twice its own length. They  
308 diminish gradually in size towards the distal region (Fig. 10 A), becoming discrete  
309 lateral projections in the pleural sheath. The last segments show sexual dimorphism,  
310 with a posterior spiracle in the eighth segment. Segments I -VII have 2 pairs of median  
311 dorsal tubercles. Abdominal segments I-II have atergum with four pairs of setae, and  
312 pleura and sternum are covered with the thoracic appendage sheaths. Abdominal  
313 segment III has a tergum and sterna with 4 pairs of setae, respectively, on each side,  
314 which are similar in shape and location to the abdominal segments IV-VII; pleura and  
315 sterna III are partially covered by the thoracic appendage sheaths (Table 2). In  
316 abdominal segments IV-VII, each tergum has 4 pairs of setae which are distributed in a  
317 similar fashion to the previous segments. Each sternum has 4 pairs of setae. In  
318 abdominal segment VIII, males and females both have two pairs of setae on the tergo,

319 and two pairs on the sternum and two pairs on the spiracle (Fig. 16F). All these are very  
320 small basiconic setae. Abdominal segment IX is covered by the larval exuvia (as is  
321 VIII), but when uncovered, sexual morphological differences can be observed. In males,  
322 there are two lobes on each side – one simple, covering the lateral lobe, and the other  
323 divided, containing the gonostylus and gonocoxite. In females, two simple and short  
324 lobes on each side – one covering the oviscapae and the other the cercus, though without  
325 setae (Fig. 17), and the genital opening sheath is discreet (Fig. 16E). Abdominal  
326 chaetotaxy can be seen in Table 2, Figs. 15 and 16.

327

328

329 **Fig 12. Scanning electron microscopy of the pupa of *Migonemyia migonei*.** A, Metathorax  
330 setae 1T (scale bar: 10  $\mu$ m); B, Proothorax setae 1P and 2P (scale bar: 20  $\mu$ m); C, Metathorax  
331 setae 3T (scale bar: 5  $\mu$ m); D, mesothorax setae 1M and 2M (scale bar: 20  $\mu$ m); E, Metathorax  
332 setae 2T (scale bar: 10 $\mu$ m). Setae numbered according to the chaetotaxy proposed in study: 1P,  
333 1T, 1M and 3T: forked-apex short trichoid sensilla (thick arrow); 2P and 2M: blunt short  
334 trichoid sensillum (thin arrow); \* campaniform sensilla.

335

336 **Fig 13. Scanning electron microscopy of the pupa of *Migonemyia migonei*.** A, head of the pupa (scale  
337 bar: 100  $\mu$ m). (B-D scale bars: 20  $\mu$ m). Setae numbered according to the chaetotaxy proposed in this  
338 study. Clypeal inferior (1), Palpal seta (2), Superior clypeal (3), Inferior frontal (4), Medial postocular (5),  
339 Internal postocular (6), External postocular (7), Medial frontal (8), Superior frontal (9), Vertical (10).

340

341 **Fig 14. Scanning electron microscopy of the pupa of *Migonemyia migonei*.** A, Pupa in lateral view.  
342 (scale bars: 200  $\mu$ m); B, Opening of pupa crest, scale from the (scale bars: 100  $\mu$ m); C, Metatorax the  
343 pupa; D, Superior spiracle pupal (C and D scale bars: 50  $\mu$ m). Abbreviations: cr: crest, mst: mesothorax,  
344 mtt: metatorax, pt: prothorax, sc: scales (hairs) of the pharate adult, sp: spiracle, tb: tubercle.



345

346 **Fig 15. Scanning electron micrograph of the pupa lateral view of *Migonemyia migonei*** .( scale bars  
 347 of A: 100  $\mu\text{m}$ , of B-D: 10  $\mu\text{m}$ ). As - abdominal segment, swv - sheath of wing venation, tb - tubercle,  
 348 black arrow - campaniform sensilla, \*increased area showing seta (1), black arrow pointing campaniform  
 349 sensilla, Internal posterior dorsal (2), External posterior dorsal (3), Laterodorsal (4).

350

351

352 **Fig 16. Scanning electron microscopy of the pupa of *Migonemyia migonei***. A, pupa ventral view; B, C  
 353 and D ventral abdominal segment of setae; E, genital opening sheath; F, part of abdominal segment 8 with  
 354 posterior spiracle. As - abdominal segment, gs - genital sheath, sp – spiracle, ss - External posterior dorsal  
 355 (3), Laterodorsal (4), External posterior ventral (6), External anterior ventral (7), Internal posterior ventral  
 356 (8).

357

358

359 **Fig. 17. Scanning electron microscopy of the pupa of *Migonimyia migonei***. A, Pupa female in ventral  
 360 view; B, Pupa male in ventral view (scale bars of A and B: 50  $\mu\text{m}$ ). s, spiracle.

361

362

363 Table 2. Chaetotaxy for pupa of *Migonemyia migonei*.

Tagma	Number	Sensillum type	Terminology
HEAD	1C	Basiconic	Clypeal inferior
	2C	Basiconic	Palpal seta
	3C	Basiconic	Clypeal superior
	4C	Basiconic	Frontal inferior
	9C	Basiconic	Frontal superior
	10C	Basiconic	Vertical
	8C	Basiconic	Frontal medial
	5C	Basiconic	Postocular medial

	6C	Basiconic	Postocular internal
	7C	Basiconic	Postocular external
THORAX			
Prothorax	1P	Basiconic	Protoracic superior
	2P	Basiconic	Prothoracic medial
	3P	Absent	Absent
Mesothorax	1M	Styloconic	Mesothoracic inferior
	2M	Styloconic	Mesothoracic medial
	3M	Absent	Absent
	4A-B M	Chaetic	Pre-alar
Metathorax	1T	Styloconic	Metathoracic internal
	2T	Styloconic	Metathoracic medial
	3T	Basiconic	Metathoracic external
	4A - B T	Basiconic	Pre-halter
ABDOMEN			
I-VII	1	Basiconic	Dorsal anterior
	2	Styloconic	Dorsal posterior internal
	3	Styloconic	Dorsal posterior external
	4	Basiconic	Laterodorsal
	8	Basiconic	Ventral posterior internal
	7	Basiconic	Ventral anterior external
	6	Basiconic	Ventral posterior external
	9	Basiconic	Ventral anterior internal
VIII	1	Basiconic	Dorsal superior
	2	Basiconic	Dorsal inferior
	3	Basiconic	Lateral
	4	Basiconic	Lateral
	5	Basiconic	
	6	Basiconic	

365        **Discussion**

366

367            The exochorion pattern of *Mg. migonei* is polygonal, and was first described by  
368 Barreto[29] , using only light microscopy and subsequently redescribed by Fausto[23]  
369 who used SEM. This polygonal pattern of exochorion sculptures is found in 28 other  
370 species of Neotropical sandflies [14,30], which are distributed in nine genera of  
371 different subtribes. This characteristic probably has a phylogenetical importance,  
372 according to the opinion of Perez & Ogosuku [31], who state that the exochorionic  
373 pattern does not reflect phylogenetic relationships based on adult characteristics. Ward  
374 and Ready [32] and Costa [33] suggested that the design of the sand fly's exochorion  
375 could be different according to the environment of the breeding site. Bahia [7] observed  
376 through SEM that the eggs of *Ny. intermedia* and *Ny. whitmani* presented a different  
377 exochorion pattern than that observed in *Mg. migonei*. Instead of presenting ornaments  
378 with polygonal reticulation, with alternating transversal rows of generally rectangular  
379 parallel cells or square to polygonal cells, the eggs of these species of *Nyssomyia*  
380 presented ornamentations that consist of parallel ridges covering the entire exochorion.  
381 This exochorion pattern was previously observed in these same species through light  
382 microscopy by Barretto [29], who described it as "connected ridges". Subsequently,  
383 Pessoa [12] described the chorion of *Ev. Carmelinoi*, and the genus *Evandromyia* is  
384 phylogenetically close to *Migonemyia*. Nevertheless, the knowledge about sand fly  
385 zootaxonomy is a little scarce.

386            The chaetotaxy and morphological structures of Neotropical phlebotomine  
387 larvae have been discussed previously by several authors [4,7,8,12,14–16,27,29,32,34–  
388 38]. The general aspect of head, the position of the mouthparts a somewhat  
389 prognathous, the peculiar shape of the egg buster, similar to a "volcanic cone" [7], the

390 body shape cylindrical, and the types of the most part of the bristles observed in *Mg.*  
391 *migonei* larvae have a similar pattern to that observed by SEM in larvae of the sand fly  
392 species *Nyssomyia intermedia* and *Ny. whitmani* [7] and also of some larvae from  
393 species grouped in the Lutzomyiina and Sergentomyiina subtribes e.g. *Lutzomyia*  
394 *longipalpis*, *Lu. cruciata*, *Ev. carmelinoi* [12], *Micropygomyia chiapanensis* larvae  
395 description [4].

396 Trichoid sensilla, of different subtypes, are the most common types found on  
397 larvae and adults of phlebotomine sand flies, among others Diptera [7,39,40]. The short  
398 and long trichoid sensilla evidenced in the present work surrounding the base of the anal  
399 lobes and on the lateral sites of the prolegs of *Mg. migonei* larvae are similar to those  
400 previously observed in the same site of *Ny. intermedia* and *Ny. whitmani* larvae [7].  
401 Other similarities in relation to the typology and the pattern of sensillary distribution  
402 were also evidenced among the larvae of these species, such as brush-like trichoid  
403 sensilla, also located in front of the egg burster and on the lateral and dorsal aspects of  
404 the body segments, trichoid sensilla on the apex of the head, short trichoid sensilla on  
405 the mouthparts and weakly brush-like trichoid sensilla inserted slightly forward and  
406 between the antennae, and long trichoid sensilla are inserted further down towards the  
407 mouthparts.

408 In addition to these sensillary types, other similar sensilla such as one apical  
409 clavate basiconic sensillum, on the apex of the antennae of the *Mg. migonei* larvae, and  
410 one clavate coeloconic sensilla and three short blunt coeloconic sensilla, implanted on  
411 the proximal region of antennae, were also evident in *Ny. intermedia*, and *Ny. whitmani*  
412 larvae [7]. The latter sensillary subtype, when observed in higher magnification by  
413 Bahia [7] in larvae of *Ny. intermedia*, showed to have wall pores (multiporous clavate  
414 coeloconic sensilla; a SW-sensillum subtype). A similar sensory subtype, presenting

415 wall pores, was also identified at the equivalent larvae site of *Lu. longipalpis*, by Pessoa  
416 [11], previously designated as "multiporous papilla". Sensilla similar to the apical  
417 clavate basiconic sensillum and the clavate coeloconic sensilla were also evidenced in  
418 the larvae antennae of the *Lu. cruciata* sand fly by Oca-Aguilar [15].

419 The antennal pattern of mature larvae of *Mg. migonei* seen under SEM was done  
420 by Pessoa [11], and the other earlier stages described here can be included in category iv  
421 of Leite and Williams [5] proposal of antennae shape. To mouthpart, it is possible to  
422 highlight the teeth of mandibles because of the position of the mandible, ordinarily  
423 described in the lateral view. The chaetotaxy the thorax of *Mg. migonei* is quite similar  
424 to *Ev. carmelinoi* and *Ev. lenti*, a genus close to *Mygonemyia*, and which was described  
425 using similar methodology. In the thorax, only the shoulder accessory b seta is evidently  
426 different, very small, bifid or trifid and, in *Mg. migonei*, it is a double the size, semi-  
427 barbed, while absent in *Ev. lenti*.

428 The anterior spiracles of the *Mg. migonei* population obtained from the Ceará  
429 State in Brazil possess a few more papillae (8-9) than those from the Mérida state in  
430 Venezuela (7)[9]. *Ev. carmelinoi* and *Ev. lenti* also have 8[12]. The number of papillae  
431 of the posterior spiracle are similar between the two populations of *Mg. migonei* and *Ev.*  
432 *carmelinoi* and *Ev. lenti*. The dorsal submedian setae 7 and 8 of the meso and  
433 metathorax and abdominal segments I-VII of *Mg. migonei* are similar in size to *Ev.*  
434 *Carmelinoi*[12], and both have the double the size of setae compared to *Ev. lenti*[12].  
435 The setae 11 and 12 of *Mg. migonei* are barbed and have the double the size of the same  
436 setae in *Ev. carmelinoi* and *Ev. lenti*[12], which in their case are simple. The last  
437 segment also has slight differences; t setae 11 in *Mg. migonei* are bigger than *Ev. Lenti*,  
438 and seta 12 in *Mg. migonei* is only half the size of its counterpart in *Ev. lenti* [12]. A

439 large campaniform sensillae present in the ventral side of each tubercle of implantation  
440 of the caudal setae had not been described before and it is duly registered here.

441 The caudal filaments evidenced in the last larval segment of *Mg. migonei* and in  
442 other sand flies, is a long subtype of trichoid sensilla, which presents multiporous wall  
443 (SW-sensilla), being classified, therefore, as an olfactory sensory structure [41,42].  
444 Olfactory sensilla presents in their superficial microstructure particular very noticeable  
445 characters: multiporous walls (SW-sensilla) or walls with longitudinal grooves (DW-  
446 sensilla) [42–44]. However, these characteristics determine the generic olfactory  
447 function. The response to which odor molecules respond to each sensilla can only be  
448 determined using electrophysiological bioassays, especially the Single Sensillum  
449 Recording coupled to Gas Chromatography (SSR-GC), Single Sensillum Recording  
450 coupled to Gas Chromatography (SSR-GC), an efficient method for isolating potential  
451 insect attractants, the action potentials of odor receptor neurons (ORNs) present in each  
452 type of olfactory sensilla can be recorded *in situ* [45]. In this sense, we highlight the  
453 great importance of carrying out previous studies by scanning electron microscopy to  
454 identify the olfactory sensilla and indicate the sensillary topography, the precise location  
455 of these sensory structures, to support the performance of bioassays with SSR-GC,  
456 facilitating the accurate orientation and targeting of the electrodes and the odours pulses  
457 tested, especially in analysis of insects with very small antennas and very covered by  
458 pilosities, such as sand flies among other Diptera, e.g.

459 Different species of sandflies have different pore patterns in their caudal  
460 filaments. *N. whitmani* larvae, for example, presents in their caudal filaments pores  
461 distributed within wall grooves, deep and not very close, whereas *Ny. intermedia*'s have  
462 more separate and superficial pores, not found in well-defined grooves [7]. *Ev. lenti*  
463 larvae have a smaller number of pores in their caudal filaments, distributed along

464 longitudinal, thin, parallel and closer ridges [11]. The caudal filaments of *Mg. migonei*  
465 larvae, in turn, presents a larger number of pores, deep, between non-parallel ridges, but  
466 that interconnect. We believe that the differences observed between the distribution  
467 patterns of the pores of the caudal filament wall may serve as important characters in  
468 future taxonomic and phylogenetic studies with larvae, for a better understanding of the  
469 evolution, of the allopatric speciation process in Phlebotominae.

470         We presented in this study the first images of the pupa emerging from the Y suture of  
471 the head, and subsequently, the pupa, by movements of contraction and inflation, ruptures  
472 the thorax in the middle of the dorsal part. There are only a few pupae from Neotropical sand  
473 fly species described in detail using 3D images of SEM, however, all the head setae, small  
474 spines, and basicornics are homologous to other Neotropical pupae described [8,13–16].  
475 Nevertheless, some minor differences can be highlighted in the thorax. The setae 1P and 2P  
476 are basicornic, 1P is bifid and stout and implanted in a tubercle. In some species, the setae 1P  
477 and 2P are styloconic, or at least one of them is, e.g., *Da. beltrani*[8], *Mg. chiapanensis*[14],  
478 *Lu. cruciata*[15], *Ny. umbratilis*[16], and this characteristic is not determinant to phylogeny  
479 for Lutzomyiina. The absence of the 3P seta in *Mg. migonei* is probably an apomorphy in this  
480 species, at least in comparison to the others discussed here in this paper. The abdominal  
481 segments I -VII have 2 pairs of median dorsal tubercles, one large and conspicuous curved  
482 backwards. *My. chiapanensis*[14] and *Lu. cruciata*[15] possess these tubercles, however they  
483 are discrete, and in *Da. beltrani*[8] and *Ny. umbratilis*[16] apparently they are not in  
484 evidence. The setae 5, absent, is present in most pupae described, except for *Ny. umbratilis*  
485 [16].

486         In the present study, the immature stages of *Mg. migonei* possess some discrete  
487 or evident structures that can be used as apomorphies for phylogenetical relationships in  
488 order to understand the evolutionary history of this species. *Migonemyia migonei* is

489 possibly a species complex [46]. It is expected that the present descriptions may  
490 contribute to the taxonomy status, at least for that of *Mg. migonei* from the Ceará  
491 population, which occurs in an important endemic area for cutaneous leishmaniasis in  
492 Brazil.

## 493 **References**

494

495 1. Galati EAB. Phlebotominae (Diptera, Psychodidae): Classification, Morphology  
496 and Terminology of Adults and Identification of American Taxa. In: Rangel E.,  
497 Shaw J. (eds) Brazilian Sand Flies. Springer, Cham. 2018. Available:  
498 <https://doi.org/10.1007/978-3-319-75544-1>

499 2. Galati E. Morfologia e terminologia de Phlebotominae (Diptera: Psychodidae).  
500 Classificação e identificação de táxons das Américas. Vol I. Apostila da Disciplina  
501 Bioecologia e Identificação de Phlebotominae do Programa de Pós-Graduação em  
502 Saúde Pública. Faculdade de Saúde Pública da Universidade de São Paulo, São  
503 Paulo. 2019; 133p. Available: [http://www.fsp.usp.br/egalati/wp-](http://www.fsp.usp.br/egalati/wp-content/uploads/2020/02/Apostila_Vol_I_2019.pdf)  
504 [content/uploads/2020/02/Apostila\\_Vol\\_I\\_2019.pdf](http://www.fsp.usp.br/egalati/wp-content/uploads/2020/02/Apostila_Vol_I_2019.pdf)

505 3. Pereira AMJ, Marialva EF, Julião GR, Pessoa FAC, Medeiros JF. Survey of sand  
506 flies (Diptera: Psychodidae: Phlebotominae) in Guajará-Mirim State Park forest  
507 reserve, near the Brazil-Bolivian border, with a description of *Pintomyia fiocruzi*, a  
508 new sand fly species. *Zootaxa*. 2019;4691: 270–278. doi:10.11646/zootaxa.4691.3.7

509 4. Leite ACR, Williams P. Description of the fourth instar larva of *Lutzomyia*  
510 *longipalpis*, under scanning electron microscopy. *Mem Inst Oswaldo Cruz*.  
511 1996;91: 571–578. doi:10.1590/S0074-02761996000500007



- 512 5. Leite ACR, Williams P. The First Instar Larva of *Lutzomyia longipalpis* (Diptera:  
513 Phlebotomidae). Mem Inst Oswaldo Cruz. 1997;92: 197–203. doi:10.1590/S0074-  
514 02761997000200011
- 515 6. Secundino NF, Pimenta PFP. Scanning electron microscopy study of the egg and  
516 immature stages of the sandflies *Lutzomyia longipalpis*. Acta Microscópica. 2000;8:  
517 33–38.
- 518 7. Bahia AC, Secundino NFC, Miranda JC, Prates DB, Souza APA, Fernandes FF, et  
519 al. Ultrastructural Comparison of External Morphology of Immature Stages of  
520 *Lutzomyia (Nyssomyia) intermedia* and *Lutzomyia (Nyssomyia) whitmani* (Diptera:  
521 Psychodidae), Vectors of Cutaneous Leishmaniasis, by Scanning Electron  
522 Microscopy. Journal of Medical Entomology. 2007;44: 903–914.  
523 doi:10.1093/jmedent/44.6.903
- 524 8. Oca-Aguilar ACMD, Rebollar-Téllez E, Ibáñez-Bernal S. Descriptions of the  
525 immature stages of *Dampfomyia (Coromyia) beltrani* (Vargas & Díaz-Nájera)  
526 (Diptera: Psychodidae), with notes on morphology and chaetotaxy nomenclature.  
527 Zootaxa. 2014;3887: 251. doi:10.11646/zootaxa.3887.3.1
- 528 9. Fausto AM, Taddei AR, Mazzini M, Maroli M. Morphology and ultrastructure of  
529 spiracles in phlebotomine sandfly larvae. Medical and Veterinary Entomology.  
530 1999;13: 101–109. doi:10.1046/j.1365-2915.1999.00146.x
- 531 10. Pessoa FAC, Queiroz RG de, Ward RD. Posterior spiracles of fourth instar larvae of  
532 four species of phlebotomine sand flies (Diptera: Psychodidae) under scanning  
533 electron microscopy. Memórias do Instituto Oswaldo Cruz. 2000;95: 689–691.  
534 doi:10.1590/S0074-02762000000500013

- 535 11. Pessoa FAC, Queiroz RG de, Ward RD. External morphology of sensory structures  
536 of fourth instar larvae of neotropical species of phlebotomine sand flies (Diptera:  
537 Psychodidae) under scanning electron microscopy. *Memórias do Instituto Oswaldo*  
538 *Cruz.* 2001;96: 1103–1108. doi:10.1590/S0074-02762001000800013
- 539 12. Pessoa FAC, Feitosa MAC, CastellónN-Bermúdez EG, Ríos-Velásquez CM, Ward  
540 RD. Immature stages of two species of *Evandromyia* (*Aldamyia*) and the systematic  
541 importance of larval mouthparts within Psychodidae (Diptera, Phlebotominae,  
542 Psychodinae). *Zootaxa.* 2008;1740: 1. doi:10.11646/zootaxa.1740.1.1
- 543 13. Leite ACR, Williams P, Santos M. The pupa of *Lutzomyia longipalpis* (Diptera:  
544 Psychodidae -Phlebotominae). *Parassitologia.* 1991;33: 477–484.
- 545 14. Oca-Aguilar ACMD, Rebollar-Téllez EA, Ibáñez-Bernal S. The immature stages  
546 of *Micropygomyia* (*Coquilletimyia*) *chiapanensis* (Dampf) (Diptera: Psychodidae,  
547 Phlebotominae). *Zootaxa.* 2016;4105: 455. doi:10.11646/zootaxa.4105.5.3
- 548 15. Montes de Oca-Aguilar AC, Rebollar-Téllez EA, Piermarini PM, Ibáñez-Bernal S.  
549 Descriptions of the Immature Stages of *Lutzomyia* (*Tricholateralis*) *cruciata*  
550 (Coquillett) (Diptera: Psychodidae, Phlebotominae). *Neotropical Entomology.*  
551 2017;46: 66–85. doi:10.1007/s13744-016-0439-1
- 552 16. Alencar RB, Justiniano SCB, Scarpassa VM. Morphological Description of the  
553 Immature Stages of *Nyssomyia umbratilis* (Ward & Frahia) (Diptera: Psychodidae:  
554 Phlebotominae), the Main Vector of *Leishmania guyanensis* Floch (Kinetoplastida:  
555 Trypanosomatidae) in the Brazilian Amazon Region. *Neotropical Entomology.*  
556 2018;47: 668–680. doi:10.1007/s13744-018-0587-6

- 557 17. Araújo Filho N. Epidemiologia da leishmaniose tegumentar na Ilha Grande, PhD  
558 Thesis, Universidade Federal do Rio de Janeiro, Rio de Janeiro, 144. 1979.
- 559 18. Rangel EF, Azevedo ACR, Andrade CA, Souza NA, Wermelinger ED. Studies on  
560 sandfly fauna (Diptera: Psychodidae) in a foci of cutaneous leishmaniasis in  
561 Mesquita, Rio de Janeiro State, Brazil. Mem Inst Oswaldo Cruz. 1990;85: 39–45.  
562 doi:10.1590/S0074-02761990000100006
- 563 19. Queiroz RG. Phlebotomine sand flies of a leishmaniasis focus in Baturité, Brazil.  
564 PhD thesis, London University. 1995; 224.
- 565 20. Torrellas A, Ferrer E, Cruz I, Lima H de, Delgado O, Rangel JC, et al. Molecular  
566 typing reveals the co-existence of two transmission cycles of American cutaneous  
567 leishmaniasis in the Andean Region of Venezuela with *Lutzomyia migonei* as the  
568 vector. Mem Inst Oswaldo Cruz. 2018;113. doi:10.1590/0074-02760180323
- 569 21. Carvalho MR de, Lima BS, Marinho-Júnior JF, Silva FJ da, Valença HF, Almeida F  
570 de A, et al. Phlebotomine sandfly species from an American visceral leishmaniasis  
571 area in the Northern Rainforest region of Pernambuco State, Brazil. Cad Saúde  
572 Pública. 2007;23: 1227–1232. doi:10.1590/S0102-311X2007000500024
- 573 22. Salomón OD, Quintana MG, Bezzi G, Morán ML, Betbeder E, Valdéz DV.  
574 *Lutzomyia migonei* as putative vector of visceral leishmaniasis in La Banda,  
575 Argentina. Acta Tropica. 2010;113: 84–87. doi:10.1016/j.actatropica.2009.08.024
- 576 23. Fausto A, Feliciangeli M, Maroli M, Mazzini M. Ootaxonomic investigation of five  
577 *Lutzomyia* species (Diptera, Psychodidae) from Venezuela. Memórias do Instituto  
578 Oswaldo Cruz. 2001;96: 197–204. doi:10.1590/S0074-02762001000200011

- 579 24. de Almeida DN, Oliveira R da S, Brazil BG, Soares MJ. Patterns of Exochorion  
580 Ornaments on Eggs of Seven South American Species of *Lutzomyia* Sand Flies  
581 (Diptera: Psychodidae). *Journal of Medical Entomology*. 2004;41: 819–825.  
582 doi:10.1603/0022-2585-41.5.819
- 583 25. Lawyer P, Killick-Kendrick M, Rowland T, Rowton E, Volf P. Laboratory  
584 colonization and mass rearing of phlebotomine sand flies (Diptera, Psychodidae).  
585 *Parasite*. 2017;24: 42. doi:10.1051/parasite/2017041
- 586 26. Arrivillaga J, Navarro J, Feliciangeli MD. Morfología y quetotaxia del tagma  
587 cefálico larval de *Lutzomyia* França 1924 (Diptera: Psychodidae): proposición de un  
588 sistema de nomenclatura. *Bol Ent Nev*. 1999;14: 1–13.
- 589 27. Ward RD. A revised numerical chaetotaxy for neotropical Phlebotomine sandfly  
590 larvae (Diptera: Psychodidae). *Systematic Entomology*. 1976;1: 89–94.
- 591 28. Marcondes CB. A proposal of generic and subgeneric abbreviations for  
592 phlebotomine sandflies (Diptera: Psychodidae: Phlebotominae) of the World.  
593 *Entomological News*. 2007;118: 351–356. doi:10.3157/0013-  
594 872X(2007)118[351:APOGAS]2.0.CO;2
- 595 29. Barretto M. Morfologia dos ovos, larvas e pupas de alguns flebótomos de São  
596 Paulo. *Anais fac. Méd. Univ. S. Paulo*. 1941;17: 357–427.
- 597 30. Alencar RB, Scarpassa VM. Morphology of the eggs surface of ten Brazilian  
598 species of phlebotomine sandflies (Diptera: Psychodidae). *Acta Tropica*. 2018;187:  
599 182–189. doi:10.1016/j.actatropica.2018.07.023

- 600 31. Perez JE, Ogusuku E. Chorion patterns on eggs of *Lutzomyia* sandflies from the  
601 Peruvian Andes. *Medical and Veterinary Entomology*. 1997;11: 127–133.  
602 doi:10.1111/j.1365-2915.1997.tb00301.x
- 603 32. Ward RD, Ready PA. Chorionic sculpturing in some sandfly eggs (Diptera,  
604 Psychodidae). *Journal of Entomology Series A, General Entomology*. 1975;50:  
605 127–134. doi:10.1111/j.1365-3032.1975.tb00101.x
- 606 33. Costa WA, Costa SM da, Rangel EF, Santos-Mallet JR dos, Serrão JE. Eggshell as a  
607 characteristic to identify *Lutzomyia* (*Nyssomyia*) *intermedia* (Lutz & Neiva, 1912)  
608 and *Lutzomyia* (*Nyssomyia*) *neivai* (Pinto, 1926) (Diptera: Psychodidae:  
609 Phlebotominae), vectors of cutaneous leishmaniasis. *Revista Pan-Amazônica de*  
610 *Saúde*. 2012;3: 19–24. doi:10.5123/S2176-62232012000100003
- 611 34. Abonnenc E. L'oeuf et les formes pré-imaginale de deux Phlébotomes africains: *P.*  
612 *antennatus* var. *occidentalis* Theodor, 1933 et *P. dubius* Parrot, Mornet et Cadenat,  
613 1945. *Arch Institut Pasteur d'Algérie*. 1956;34: 518–539.
- 614 35. Hanson W. The immature stages of the subfamily Phlebotominae in Panama  
615 (Diptera: Psychodidae) PhD Thesis, Ann Arbor, University of Kansas, Michigan.  
616 1968; 105.
- 617 36. Lane RP, El Sawaf B. The Immature Stages of *Phlebotomus Langeroni* (Diptera:  
618 Psychodidae)1. *Journal of Medical Entomology*. 1986;23: 263–268.  
619 doi:10.1093/jmedent/23.3.263
- 620 37. Carzola D, Oviedo M. Quetotaxia del IV estadio larval de *Lutzomyia* (*Nyssomyia*)  
621 *hernandezi* (Diptera: Psychodidae, Phlebotominae). *Revista Colombiana de*  
622 *Entomología*. 2001.

- 623 38. Carzola D, Oviedo M. Ultrastructural aspects of immature stages of *Micropygomyia*  
624 (*Sauromyia*) *trinidadensis* (Diptera: Psychodidae, Phlebotominae). Saber,  
625 Universidad de Oriente. 2015;27: 232–241.
- 626 39. Fernandes F de F, Bahia AC, Secundino NFC, Pimenta PFP. Ultrastructural  
627 Analysis of Mouthparts of Adult Horn Fly (Diptera: Muscidae) From the Brazilian  
628 Midwest Region. Geden C, editor. Journal of Medical Entomology. 2020; tjaa085.  
629 doi:10.1093/jme/tjaa085
- 630 40. Fernandes FF, Barletta A, Orfanó A, Pinto LC, Pimenta R, Miranda JC, et al.  
631 Ultrastructure of the antennae and sensilla of *Nyssomyia intermedia* (Diptera:  
632 Psychodidae), vector of American cutaneous leishmaniasis. J Med Entomol. 2020;  
633 1–10.
- 634 41. Zacharuk R. Antennae and sensilla, pp. 1-69. In G. A. Kerkut and L. I. Gilbert  
635 (eds.), Comprehensive insect physiology, biochemistry and pharmacology.  
636 Pergamon, Oxford, United Kingdom. 1985.
- 637 42. Steinbrecht R. Olfactory receptors, pp. 155–176. In E. Eguchi and Y. Tominaga  
638 (eds.), Atlas of arthropod sensory receptors: dynamic morphology in relation to  
639 function. Springer, Tokyo, Japan. 1999.
- 640 43. Hallberg E, Hansson BS, Löfstedt C. Sensilla and proprioceptors, pp. 267–288. In  
641 N. Christensen (ed.), Handbook of zoology: lepidoptera, moths and butterflies, vol.  
642 2: morphology, physiology, and development. De Gruyter, Berlin, Germany. 2003.
- 643 44. Shanbhag S, Müller B, Steinbrecht R. Atlas of olfactory organs of *Drosophila*  
644 *melanogaster* 1. Types, external organization, innervation and distribution of  
645 olfactory sensilla. Int. J. Insect. Morphol. Embryol. 1999;28: 337–397.

- 646 45. Ghaninia M, Larsson M, Hansson BS, Ignell R. Natural odor ligands for olfactory  
647 receptor neurons of the female mosquito *Aedes aegypti*: use of gas chromatography-  
648 linked single sensillum recordings. *Journal of Experimental Biology*. 2008;211:  
649 3020–3027. doi:10.1242/jeb.016360
- 650 46. Costa PL, Brazil RP, Fuzari AA, Latrofa MS, Annoscia G, Tarallo VD, et al.  
651 Morphological and phylogenetic analyses of *Lutzomyia migonei* from three  
652 Brazilian states. *Acta Tropica*. 2018;187: 144–150.  
653 doi:10.1016/j.actatropica.2018.07.027
- 654

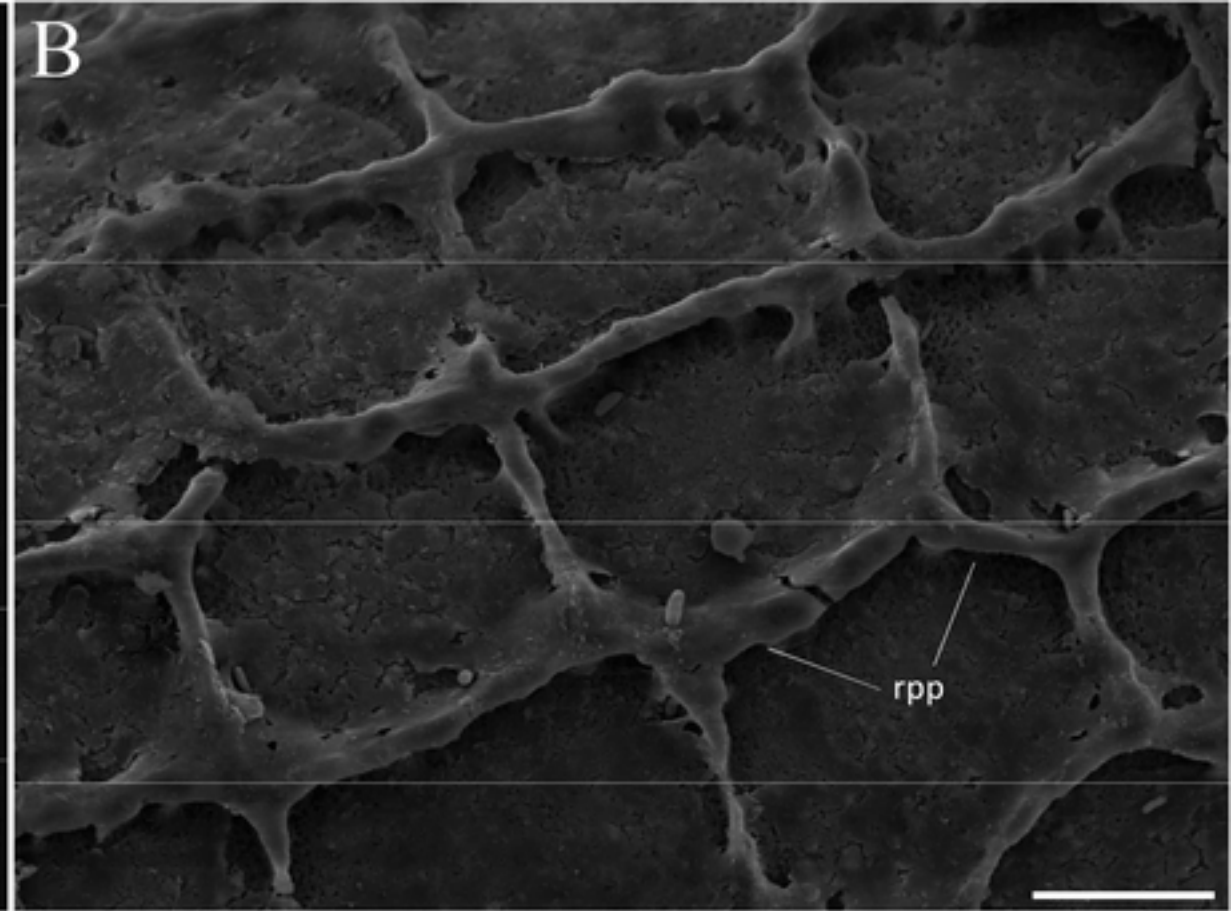
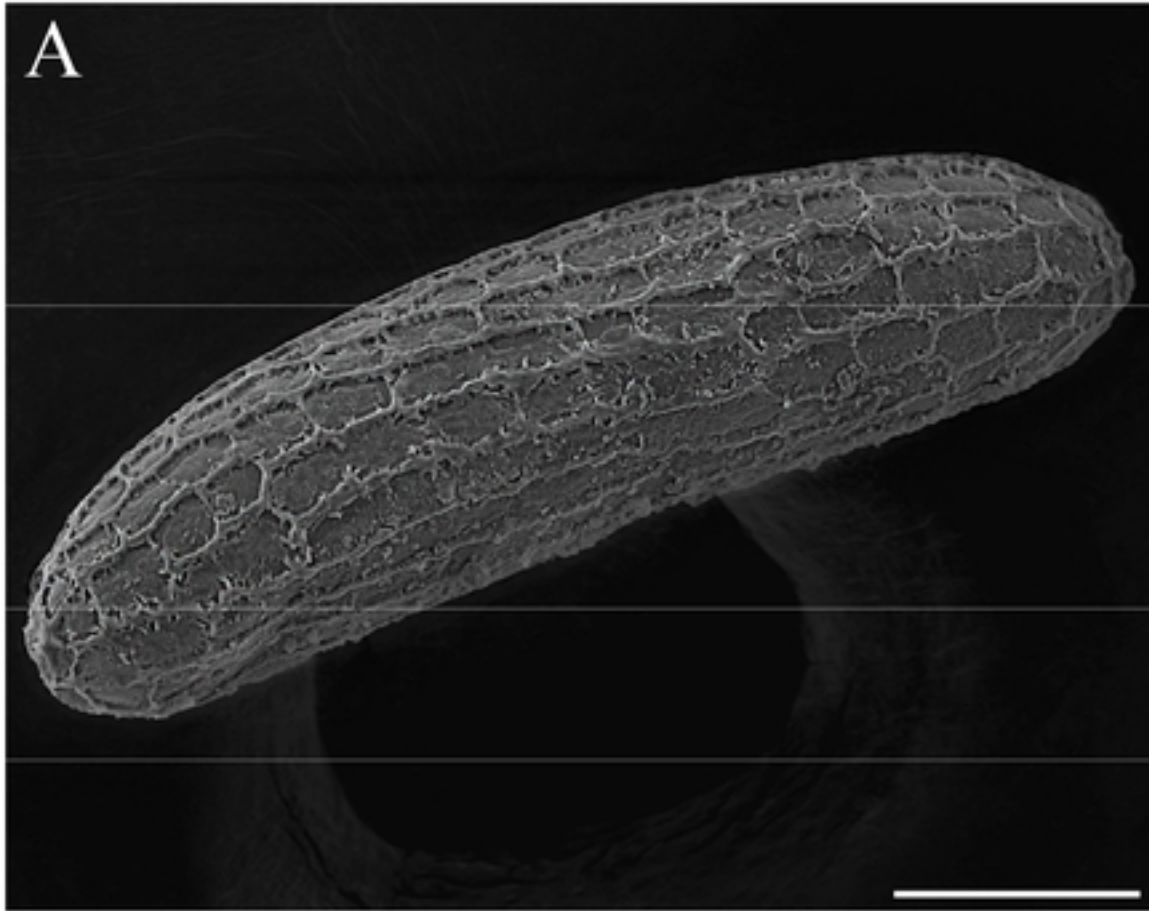
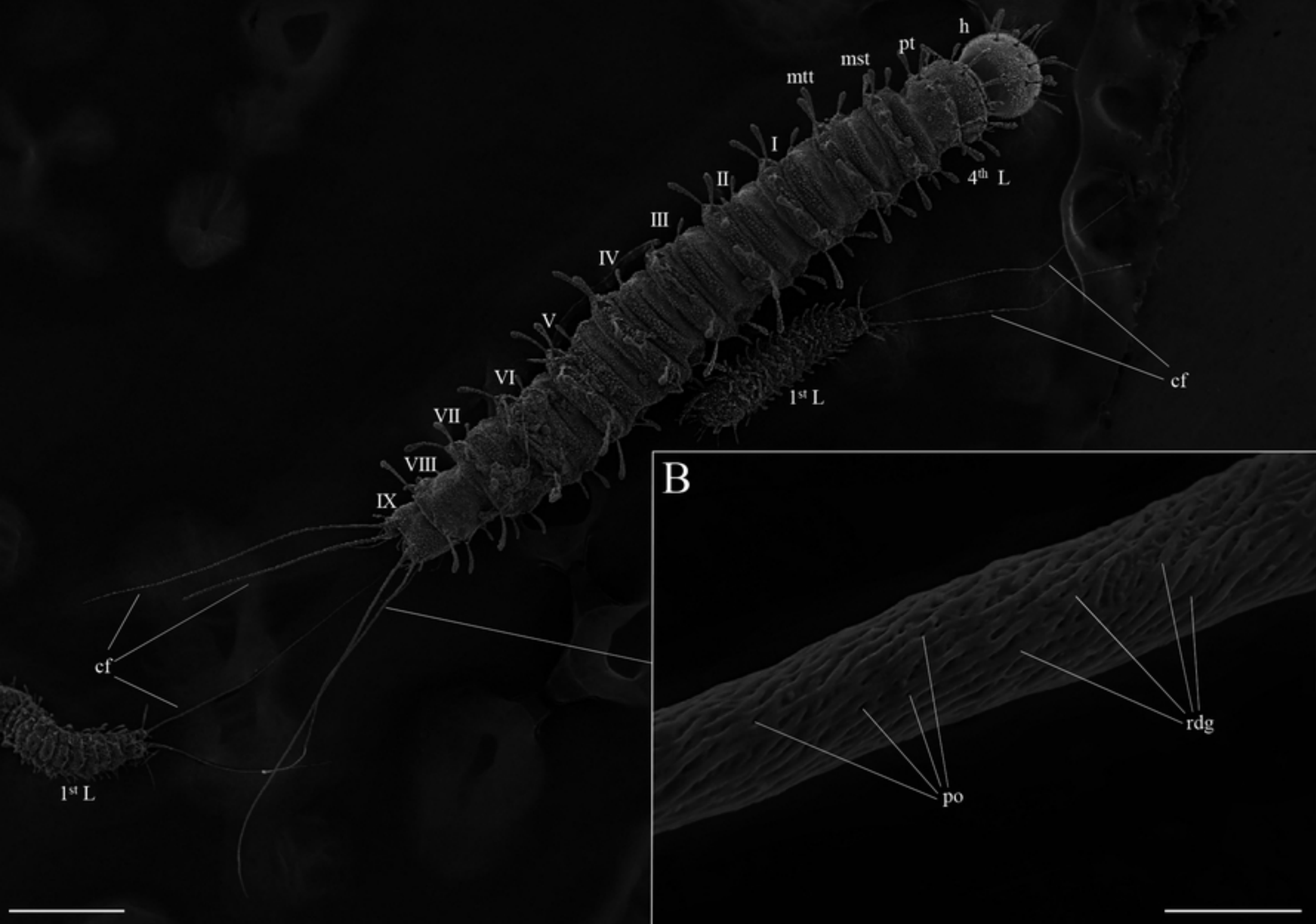


Figure 1



A



B

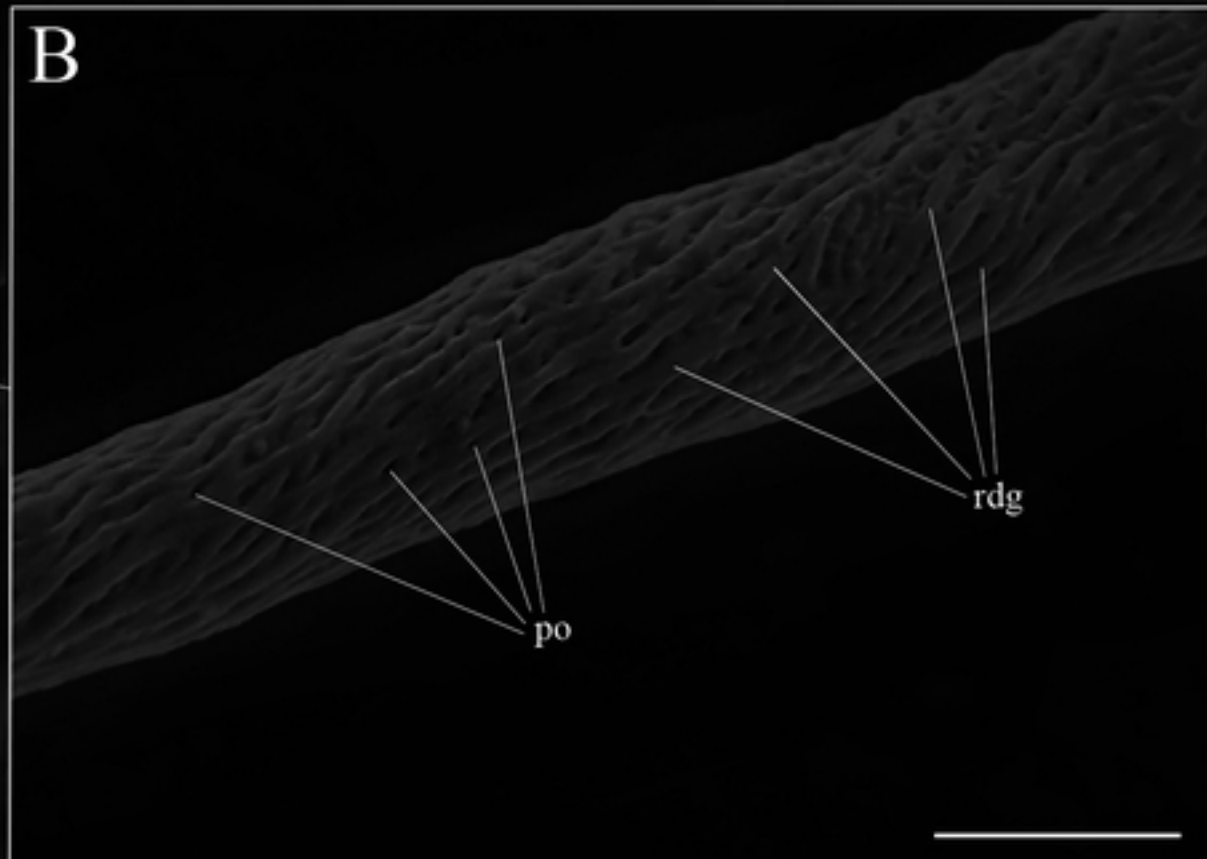


Figure 2

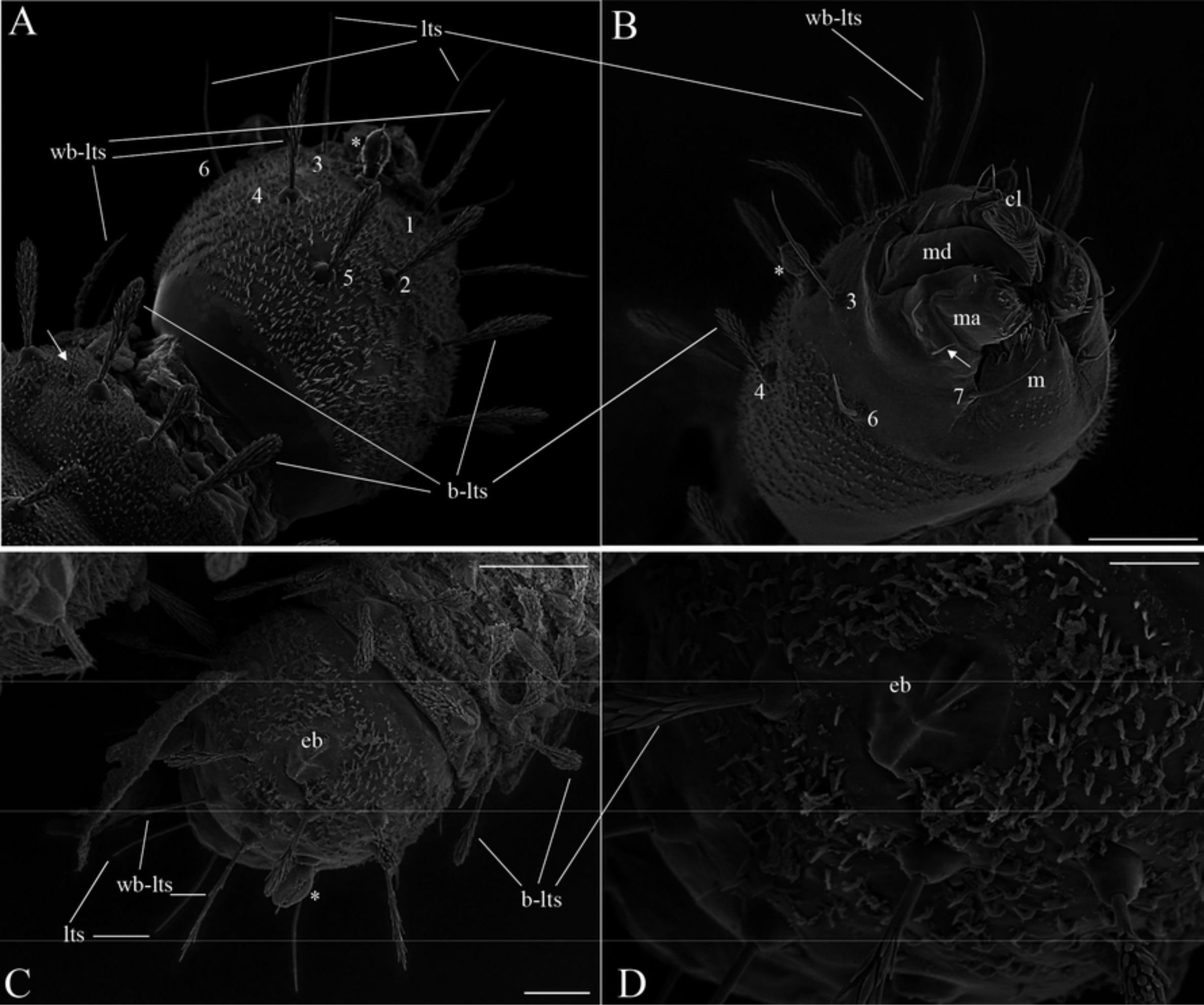


Figure 3

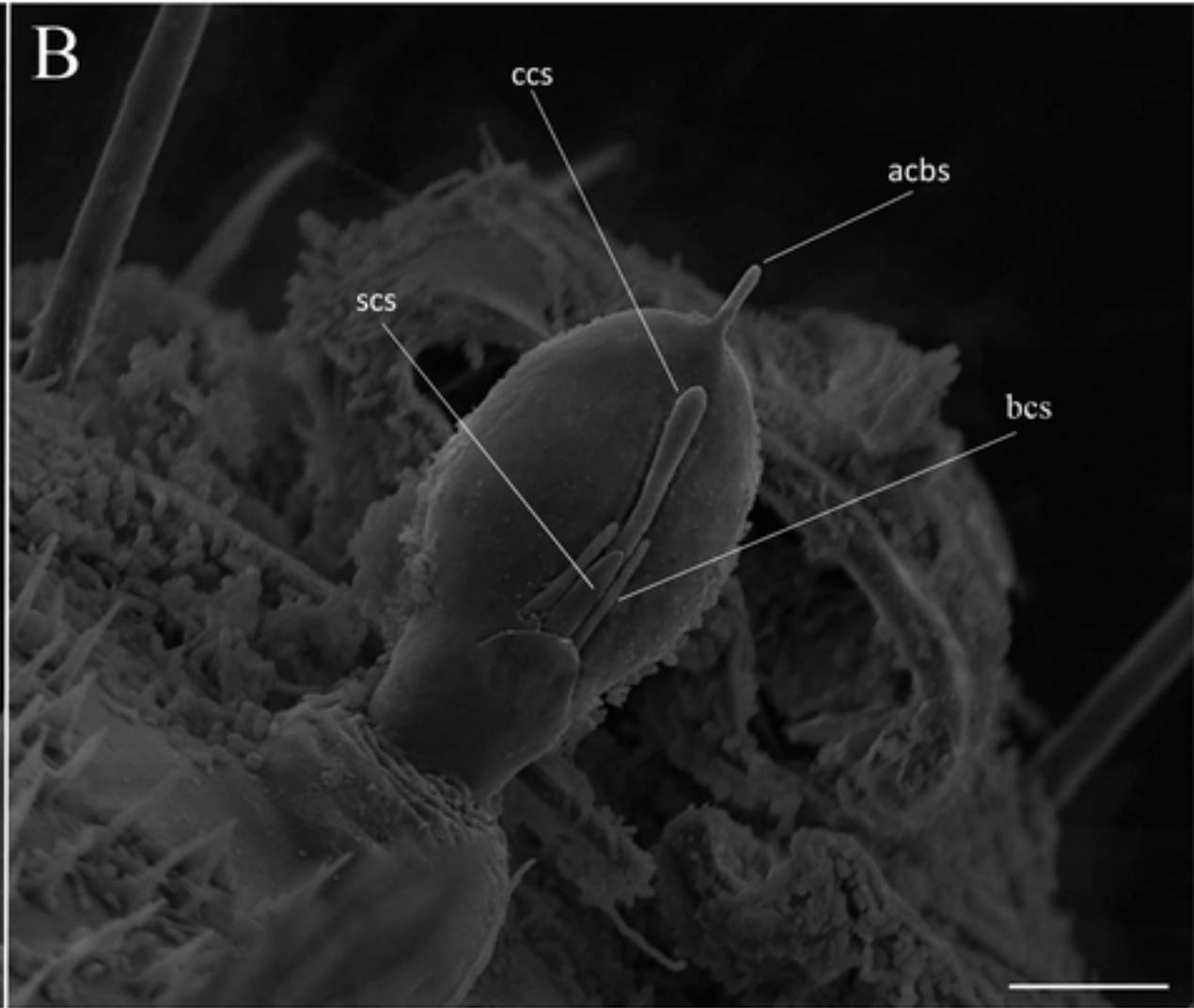
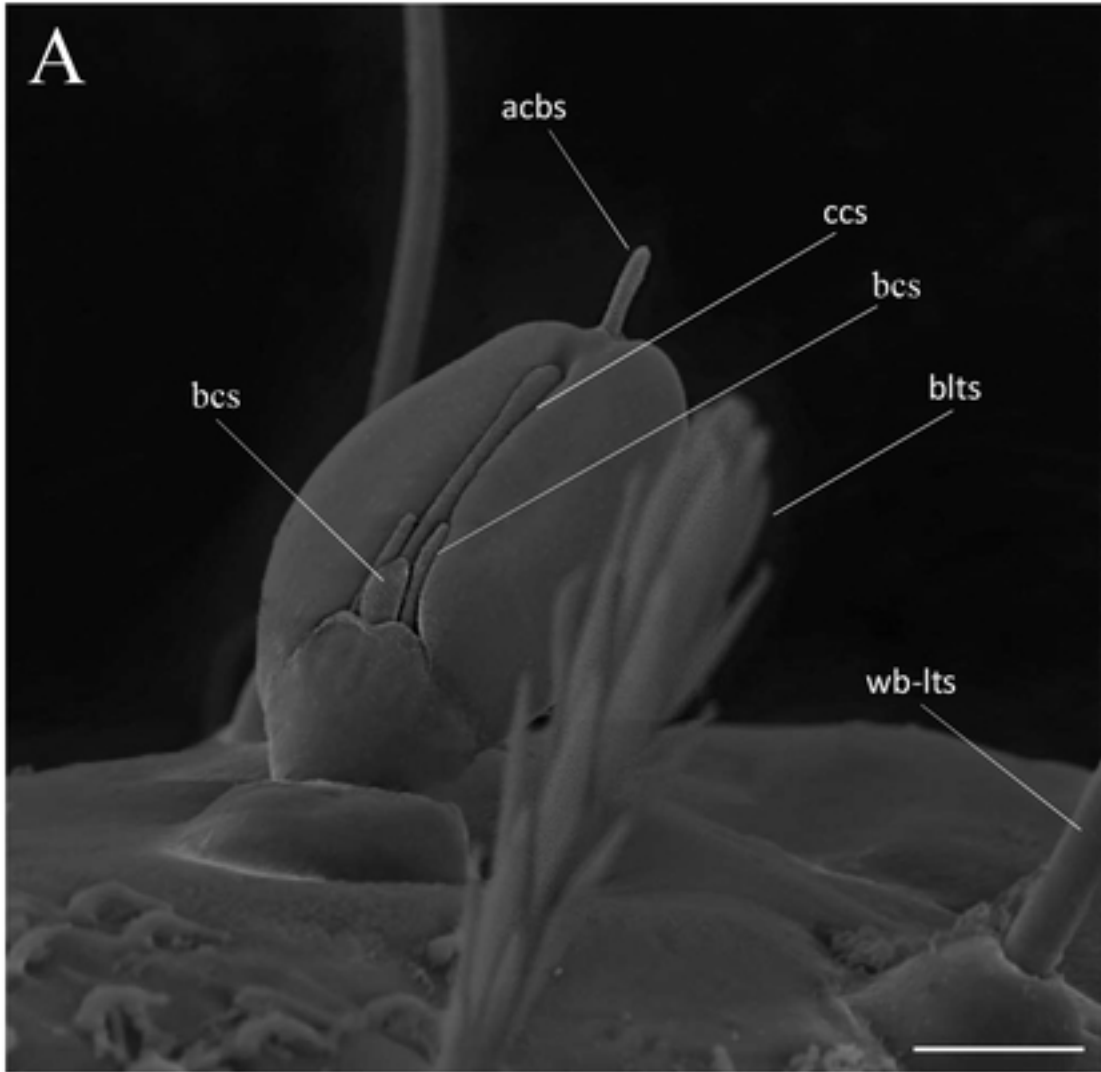


Figure 4

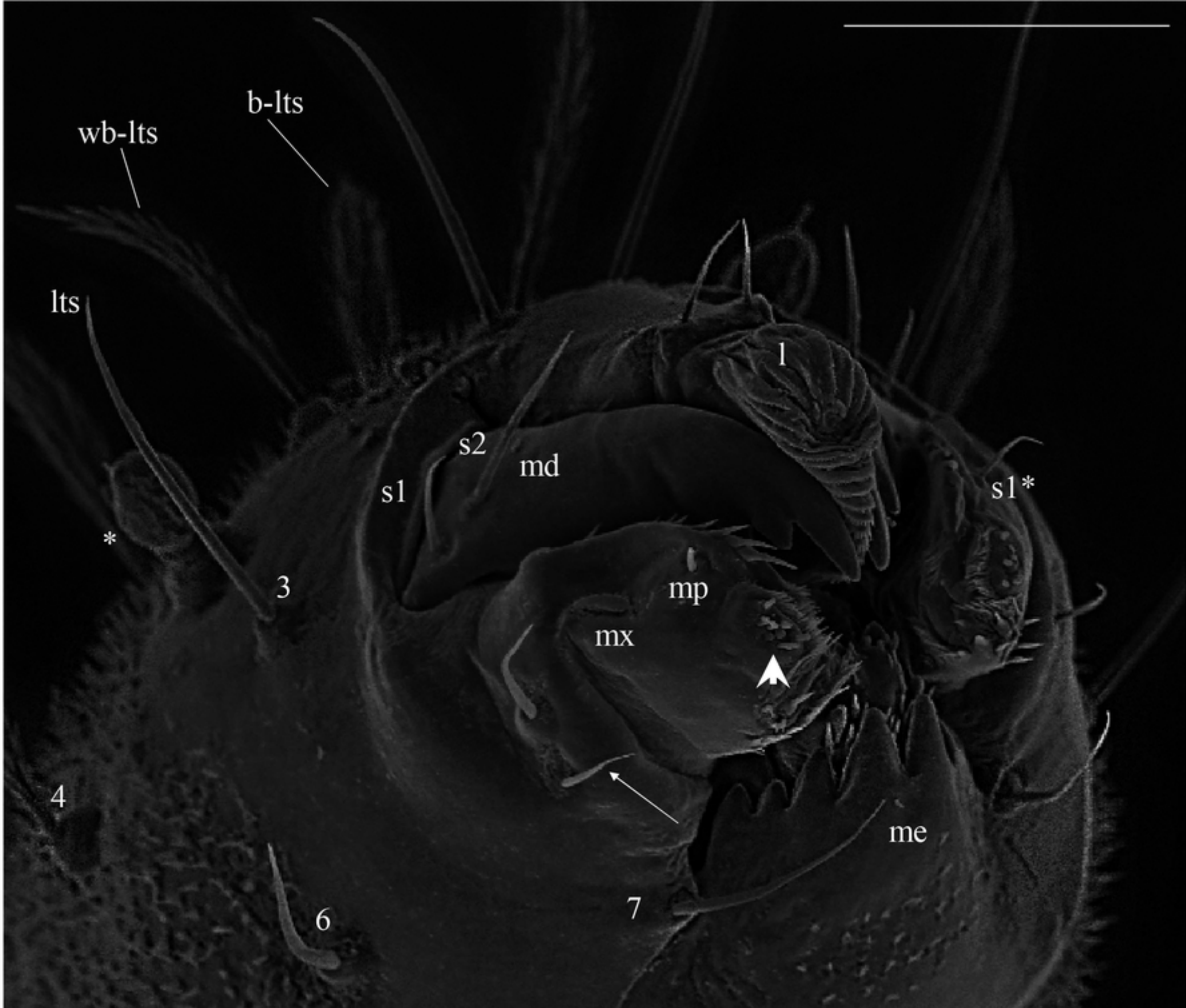


Figure 5

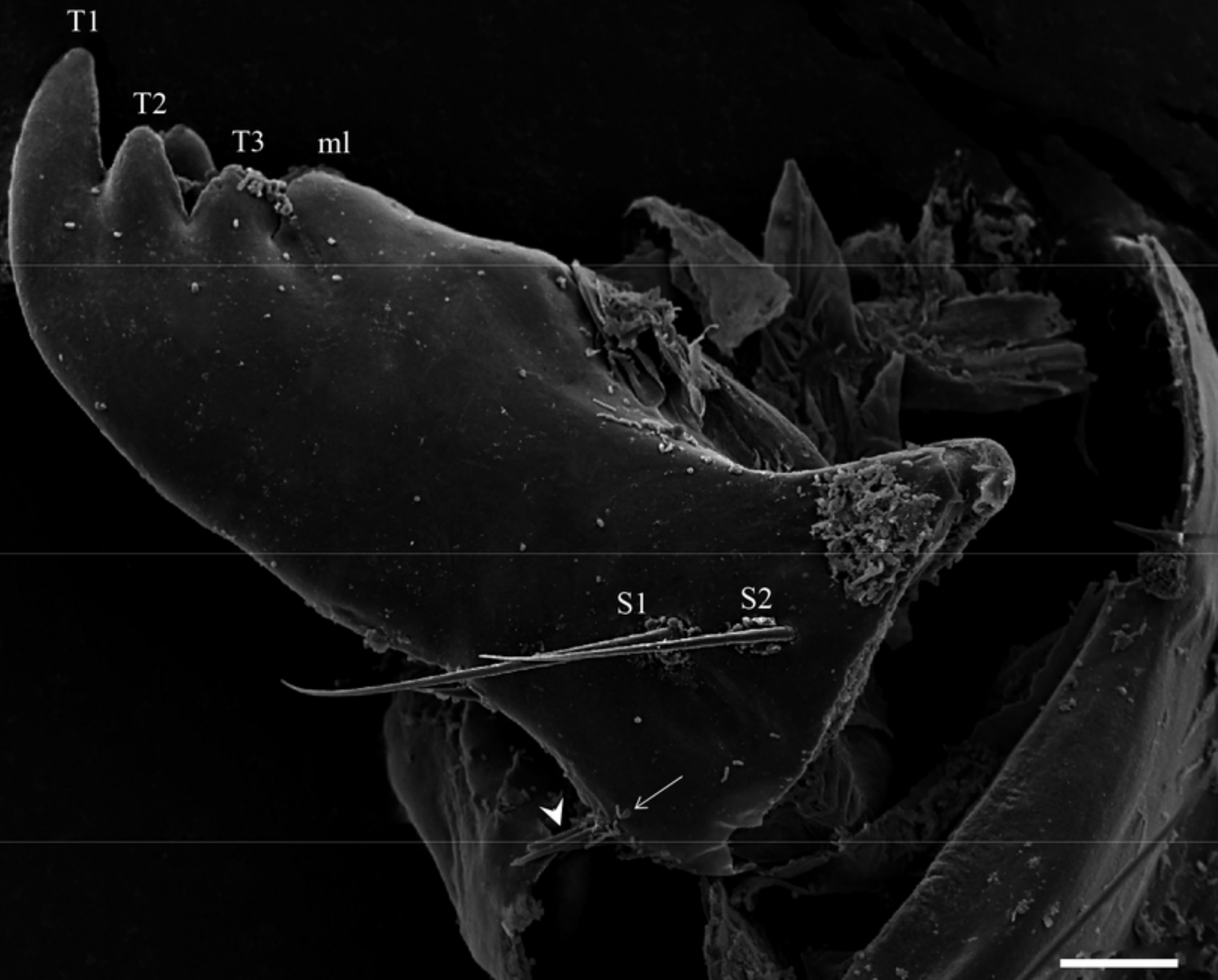


Figure 6

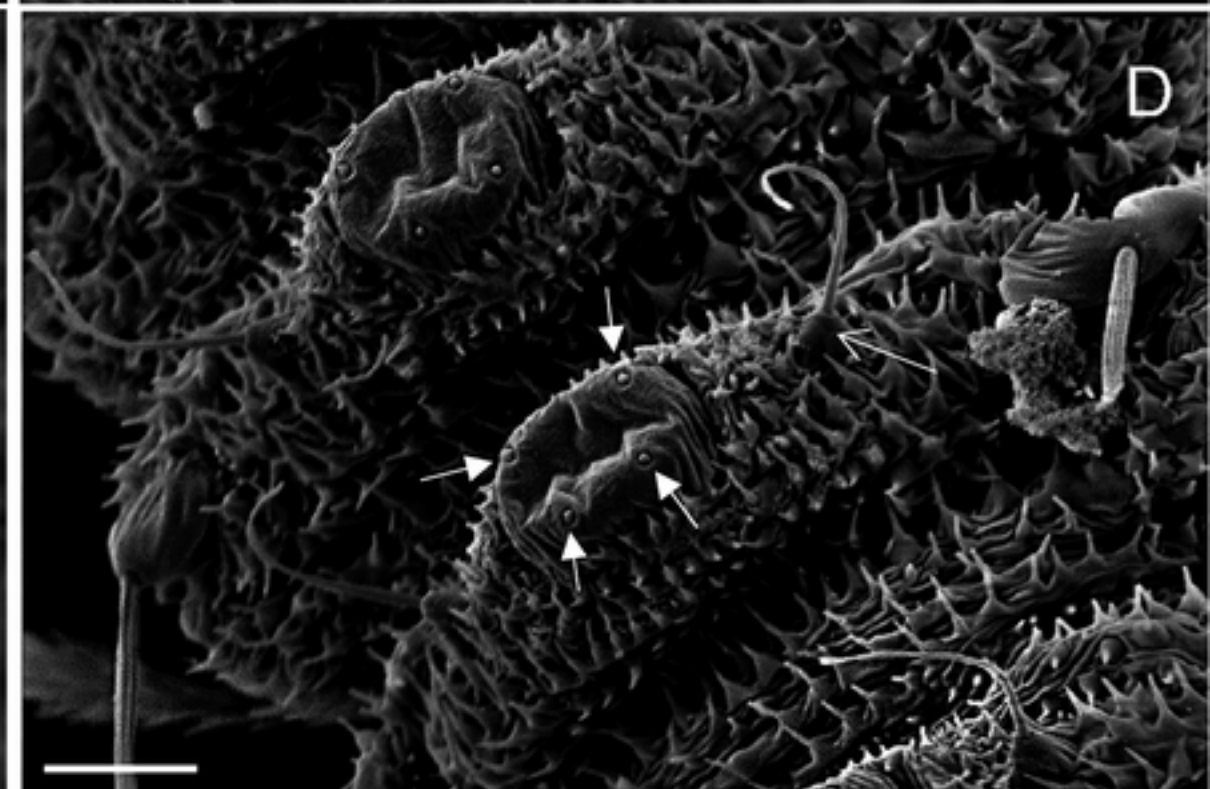
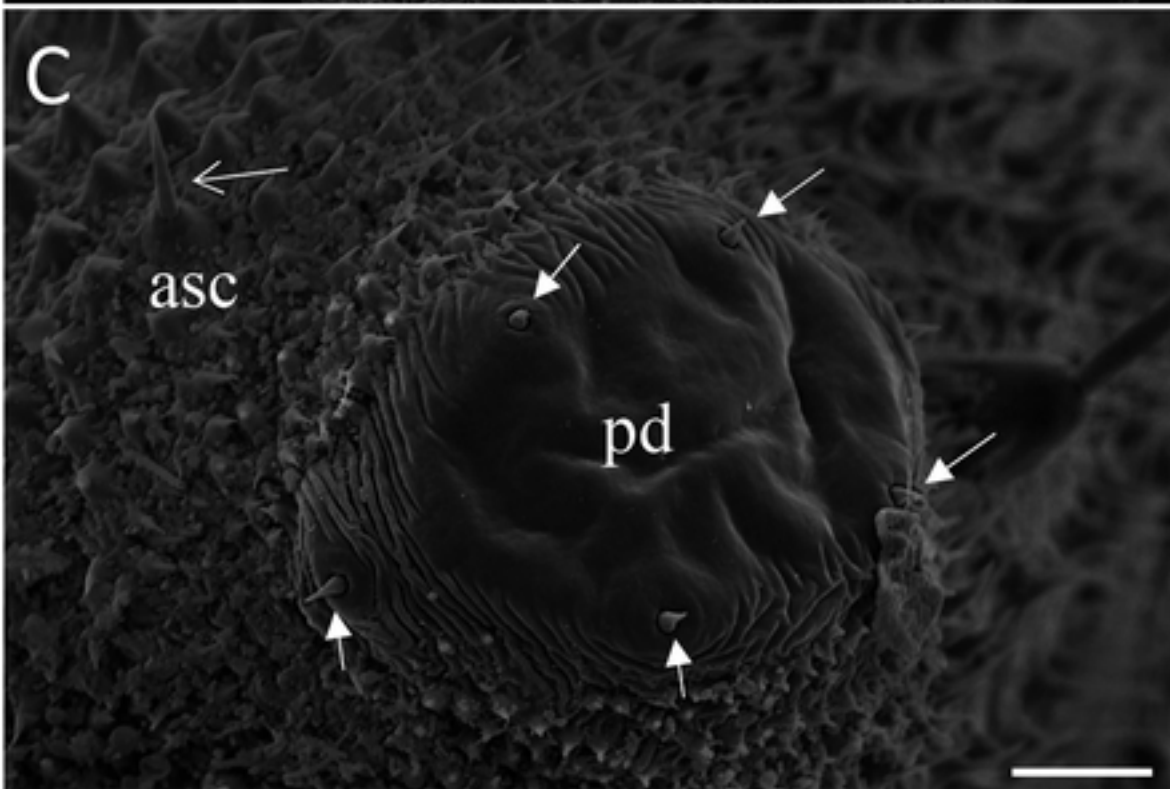
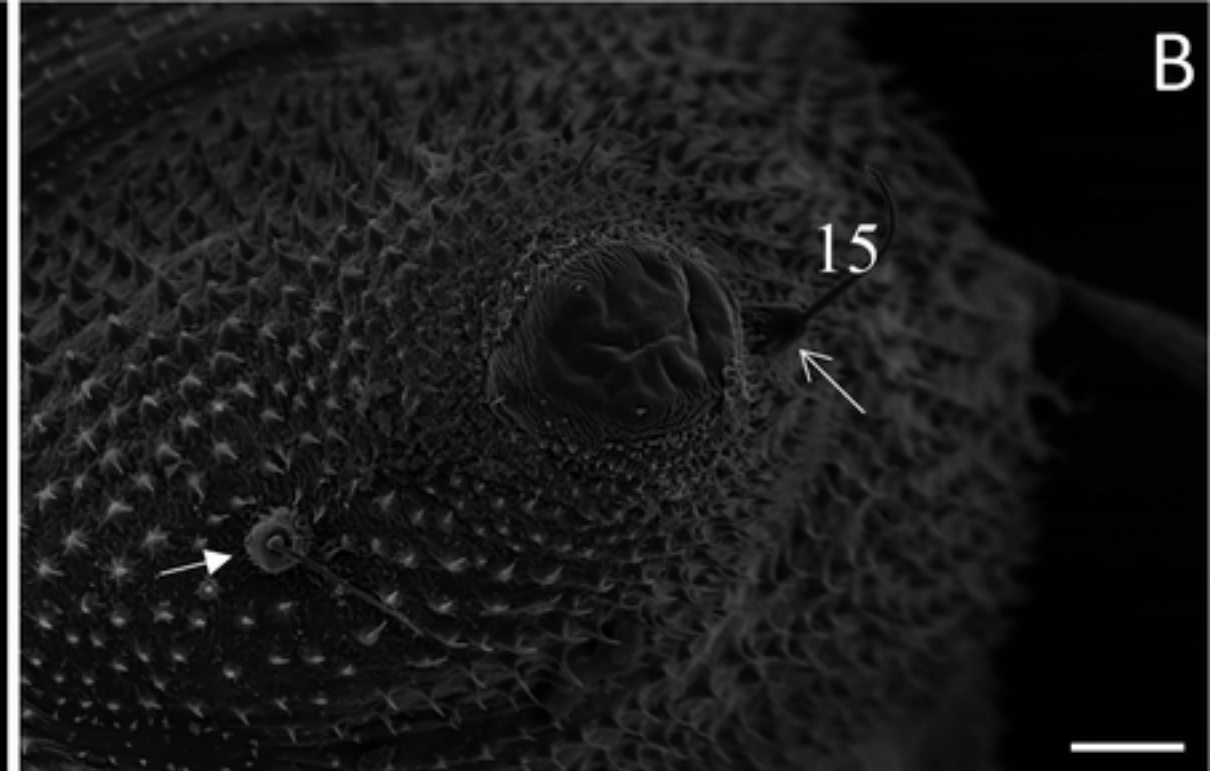
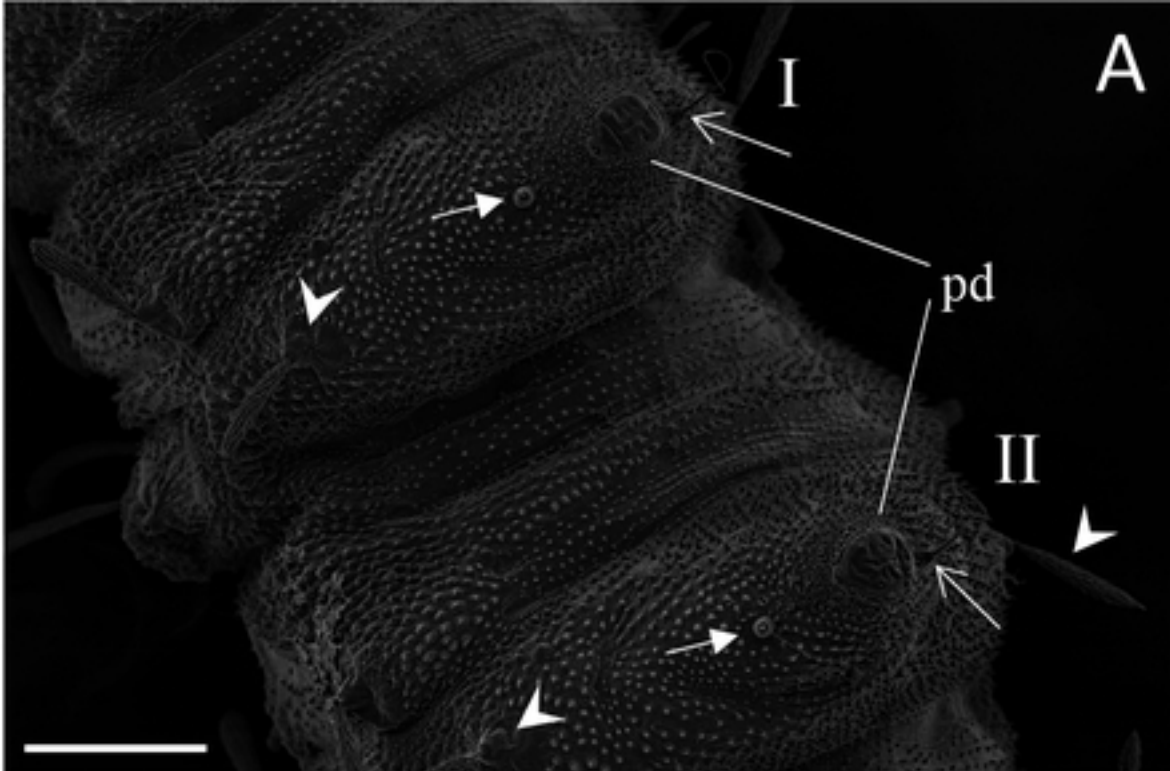


Figure 7

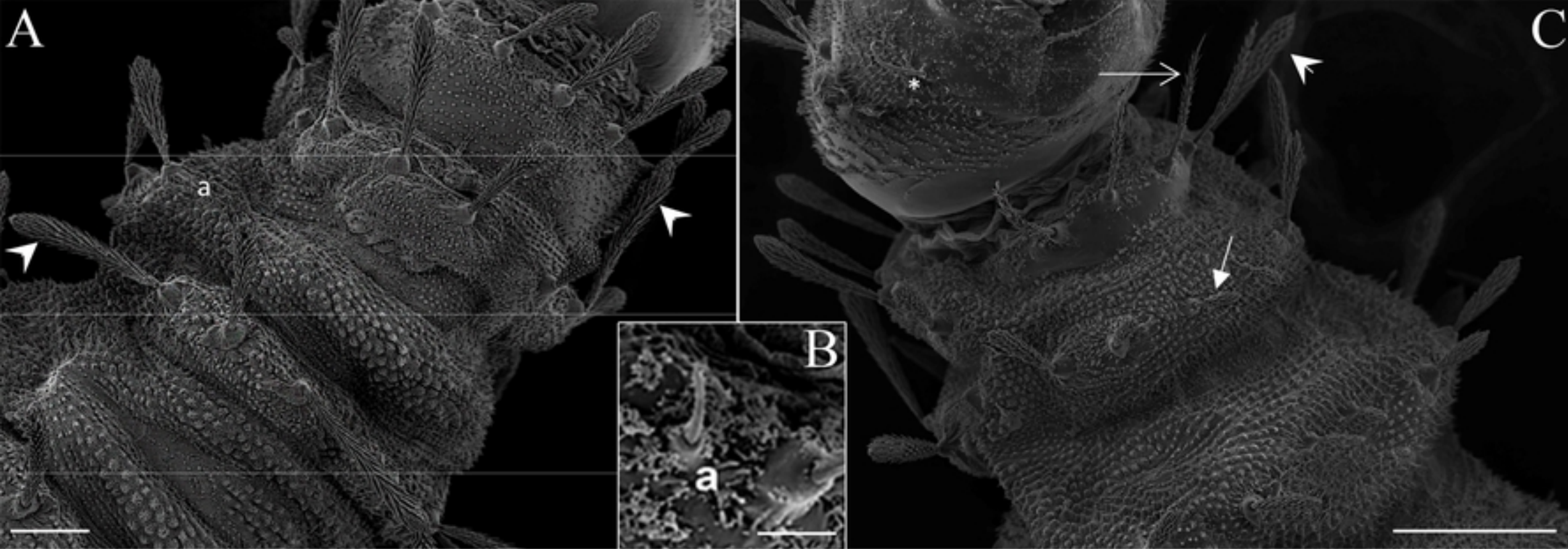


Figure 8

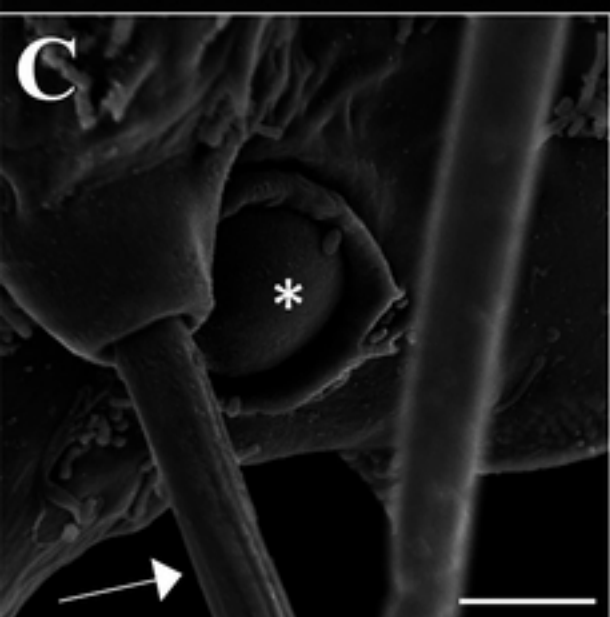
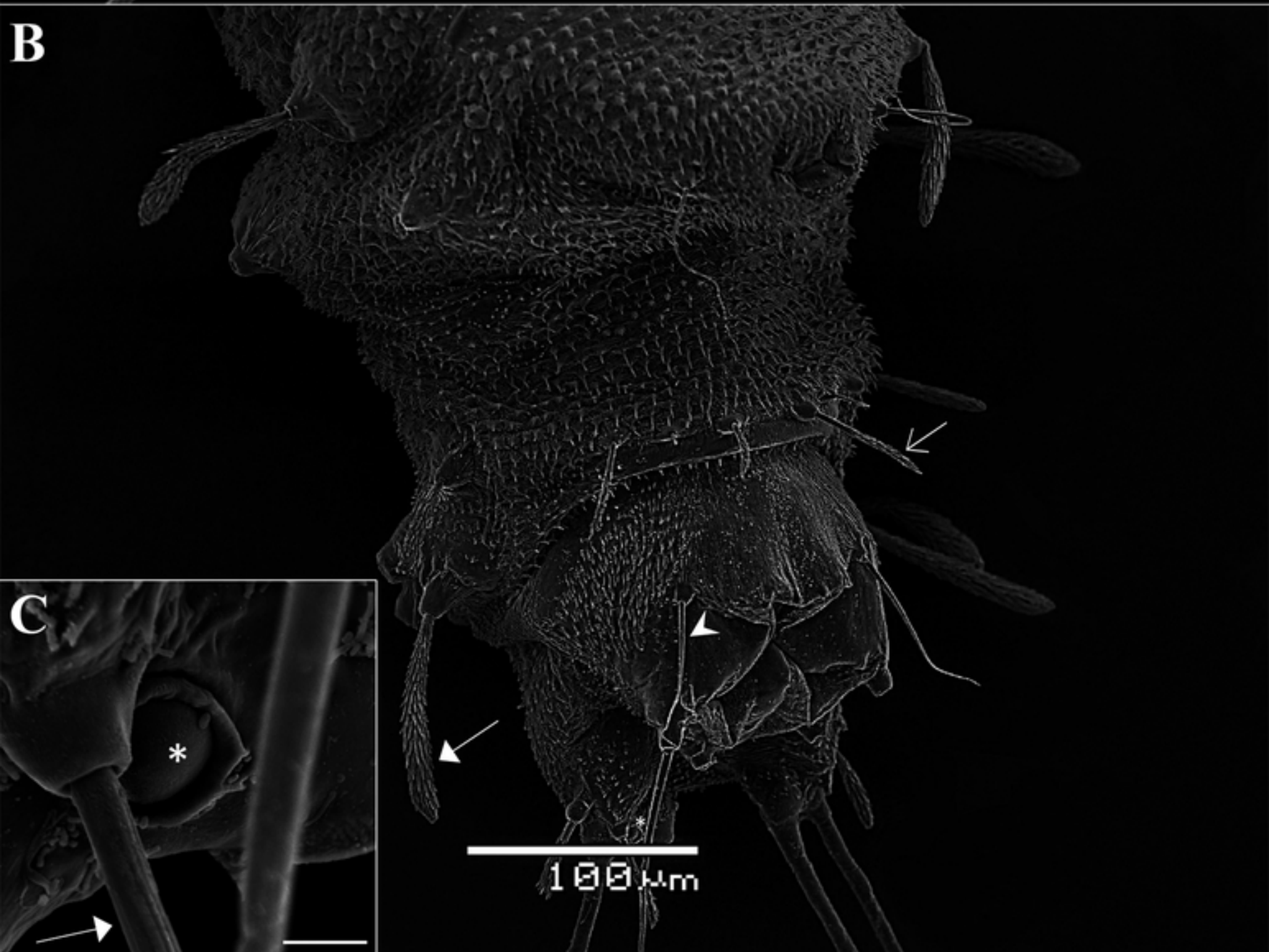
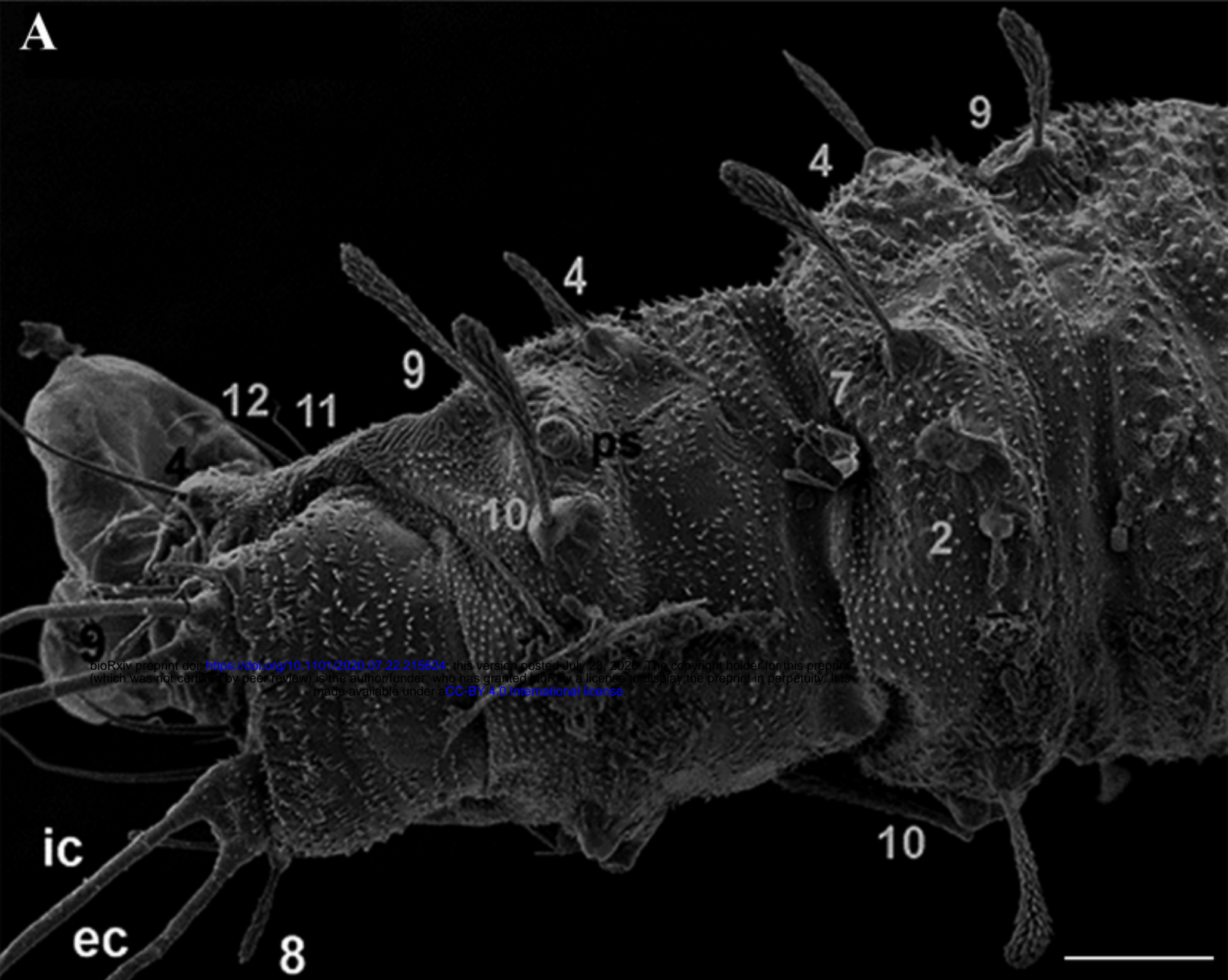


Figure 9



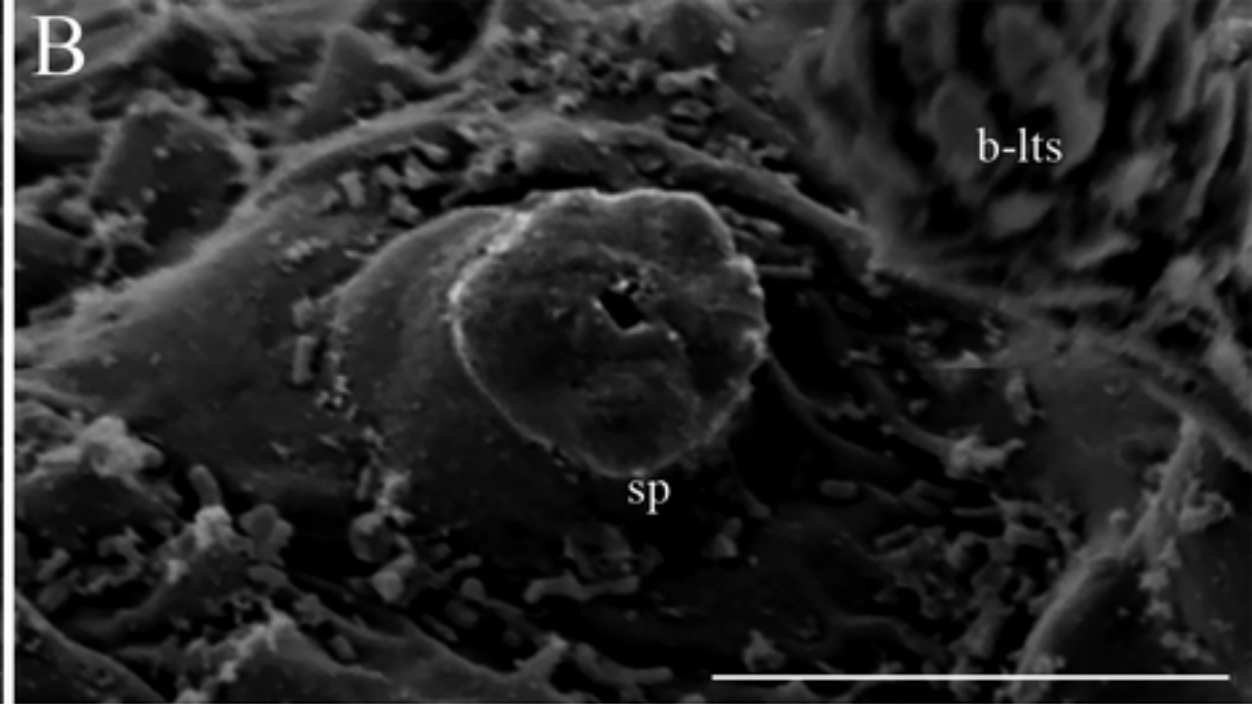
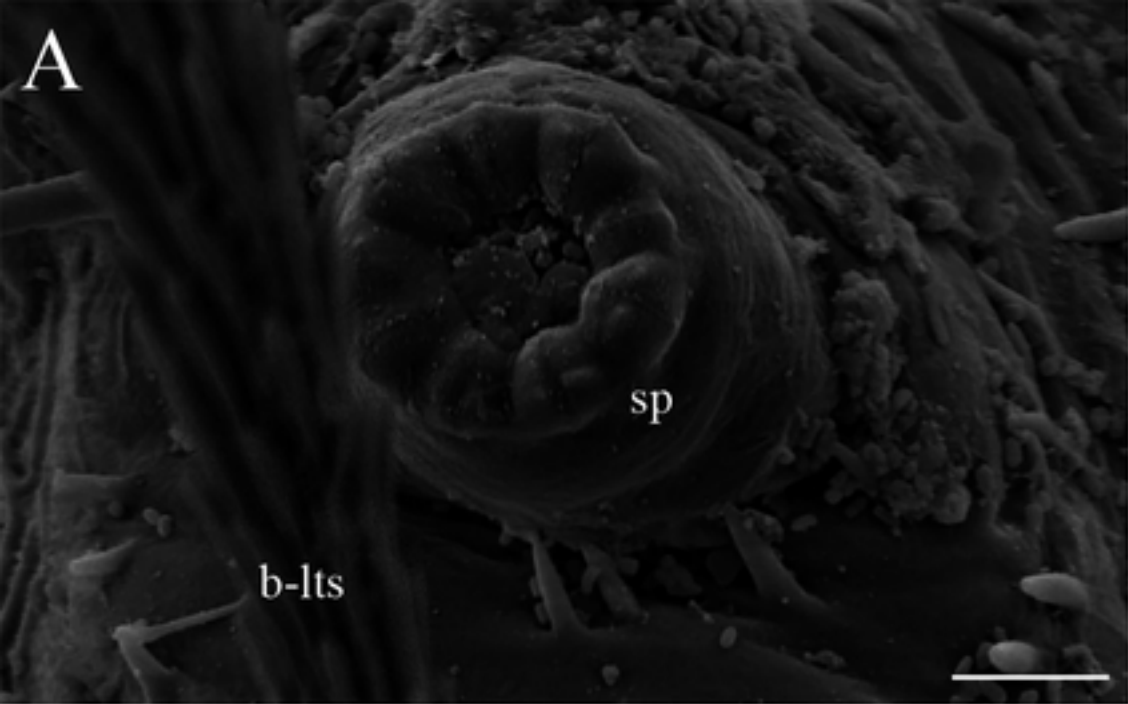


Figure 10



Figure 11

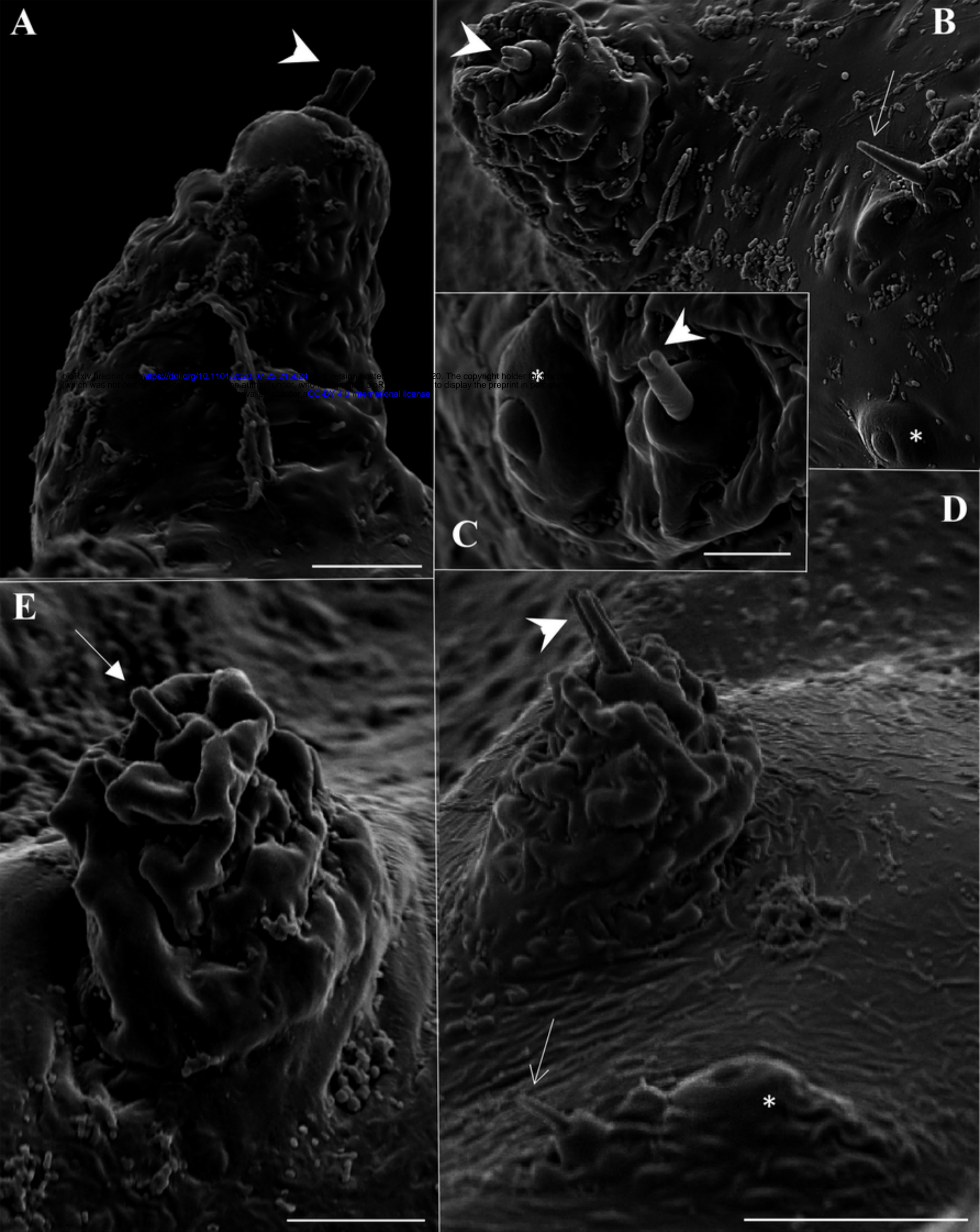


Figure 12

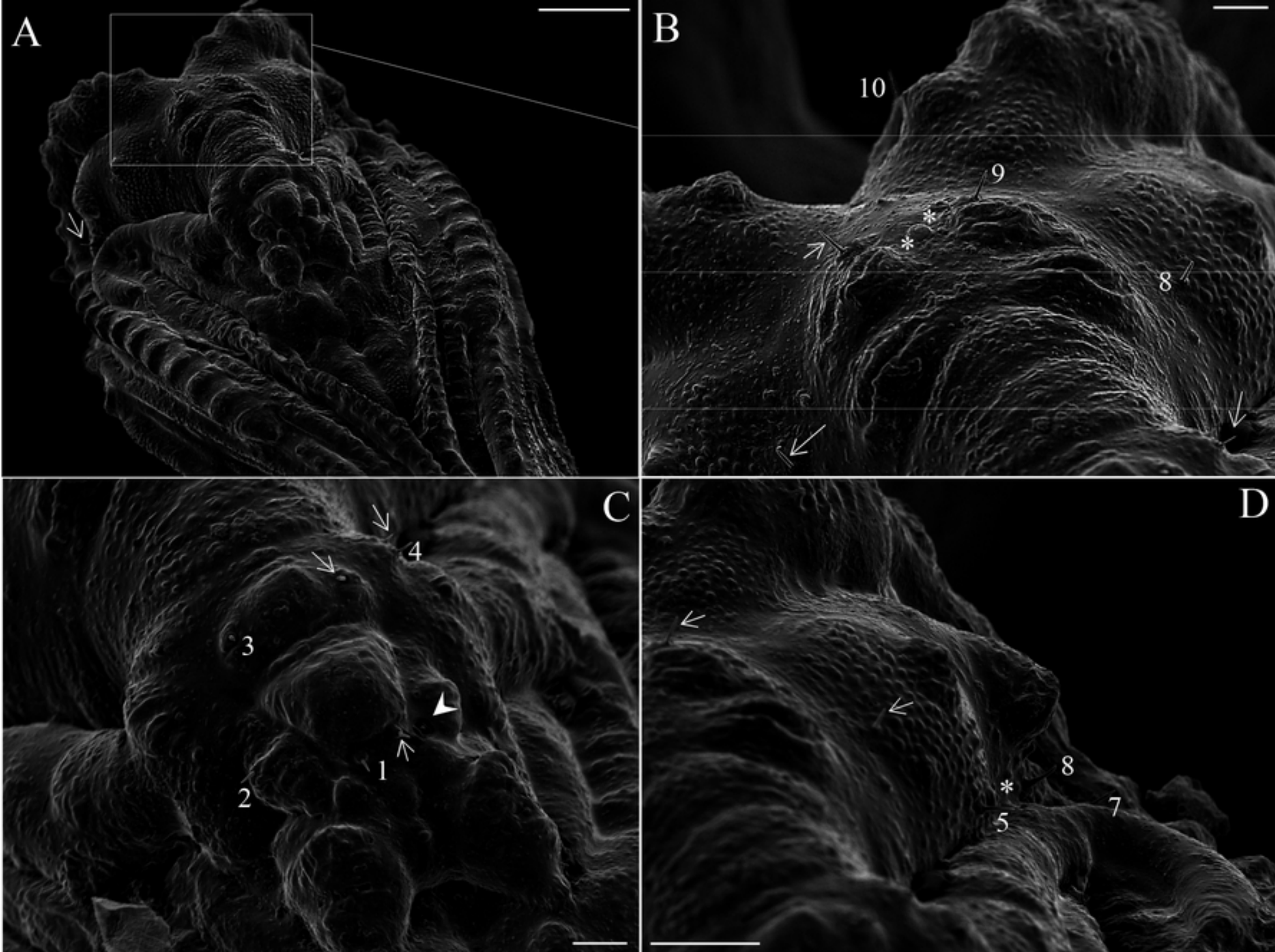


Figure 13

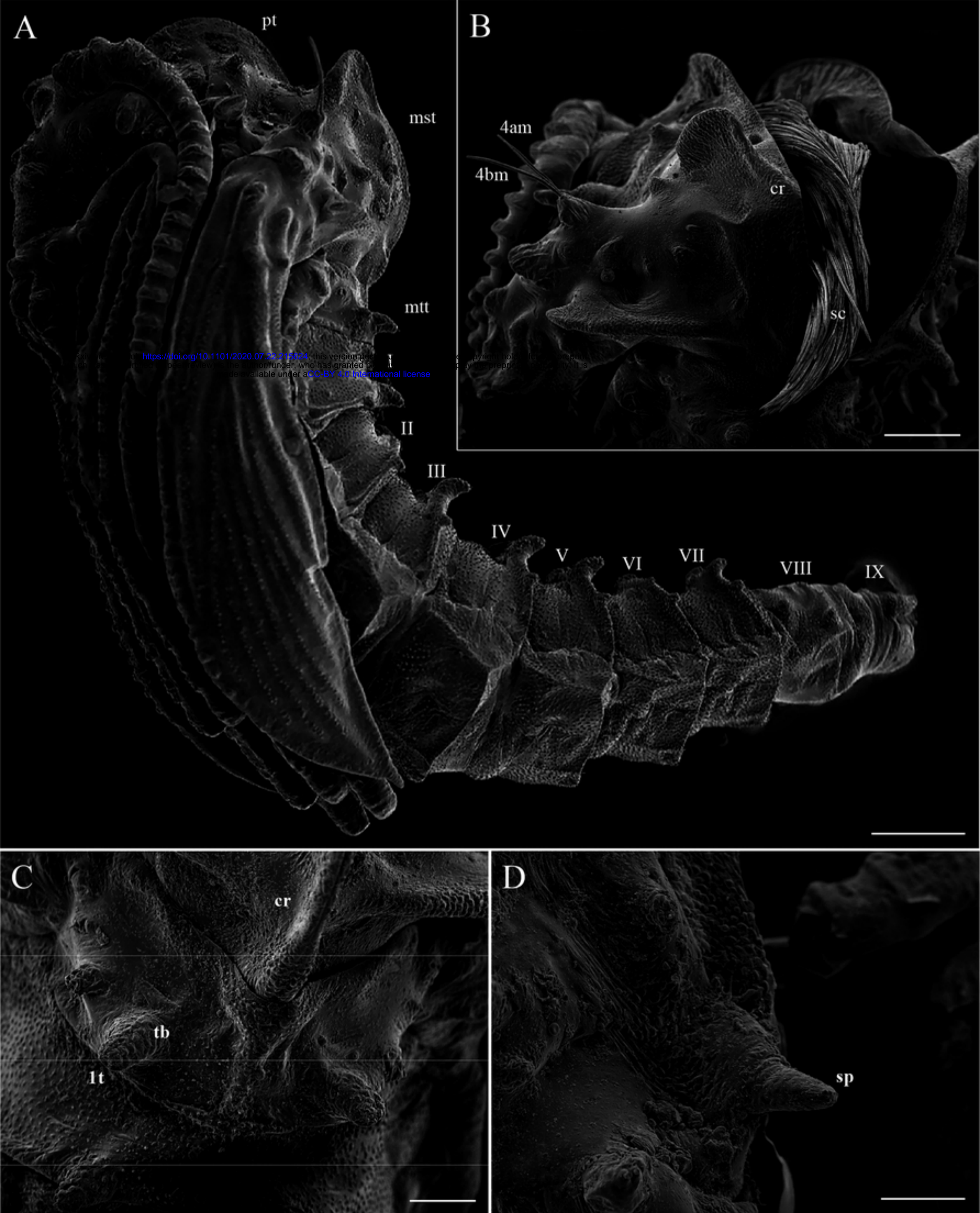


Figure 14

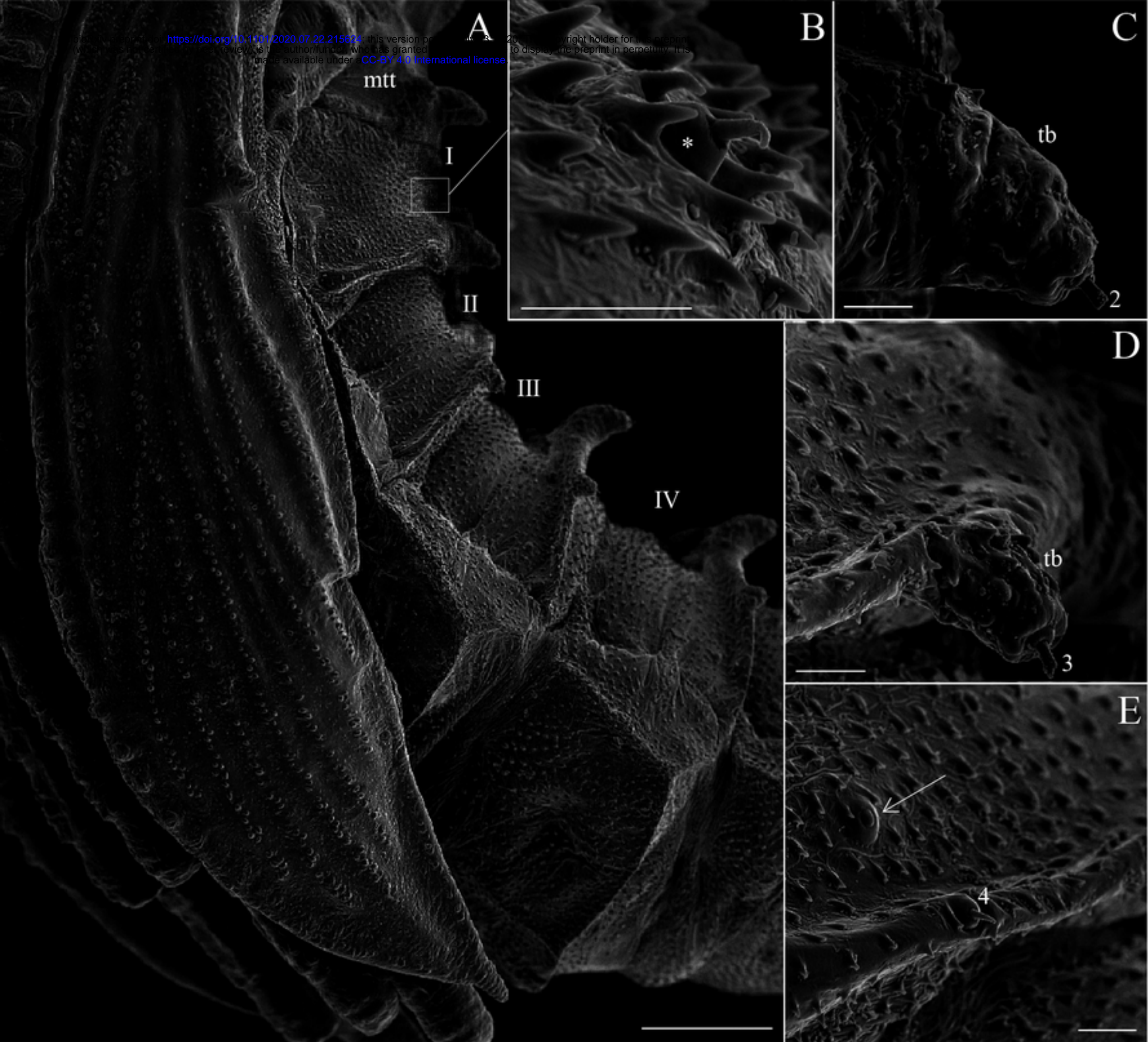


Figure 15

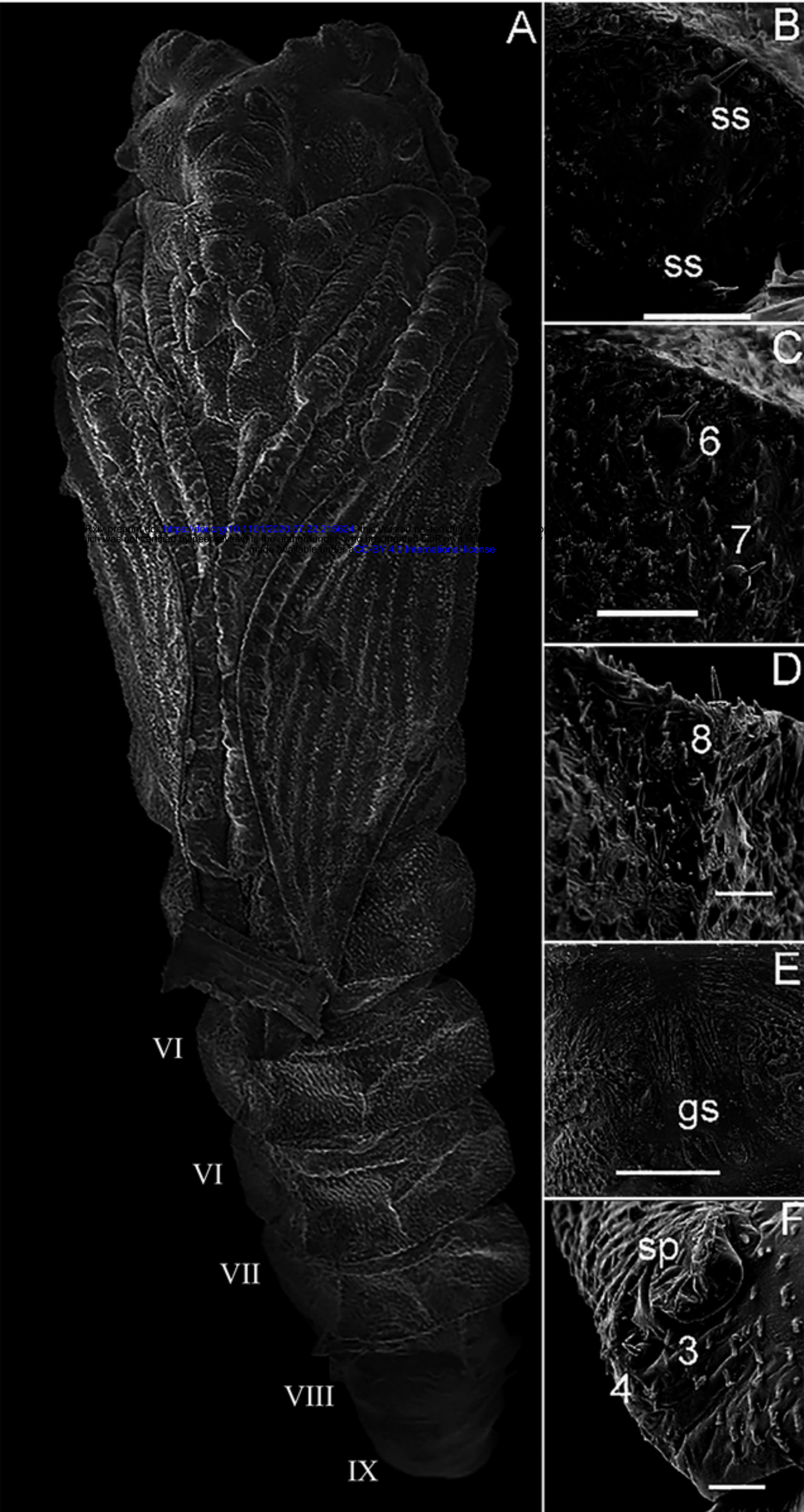


Figure 16

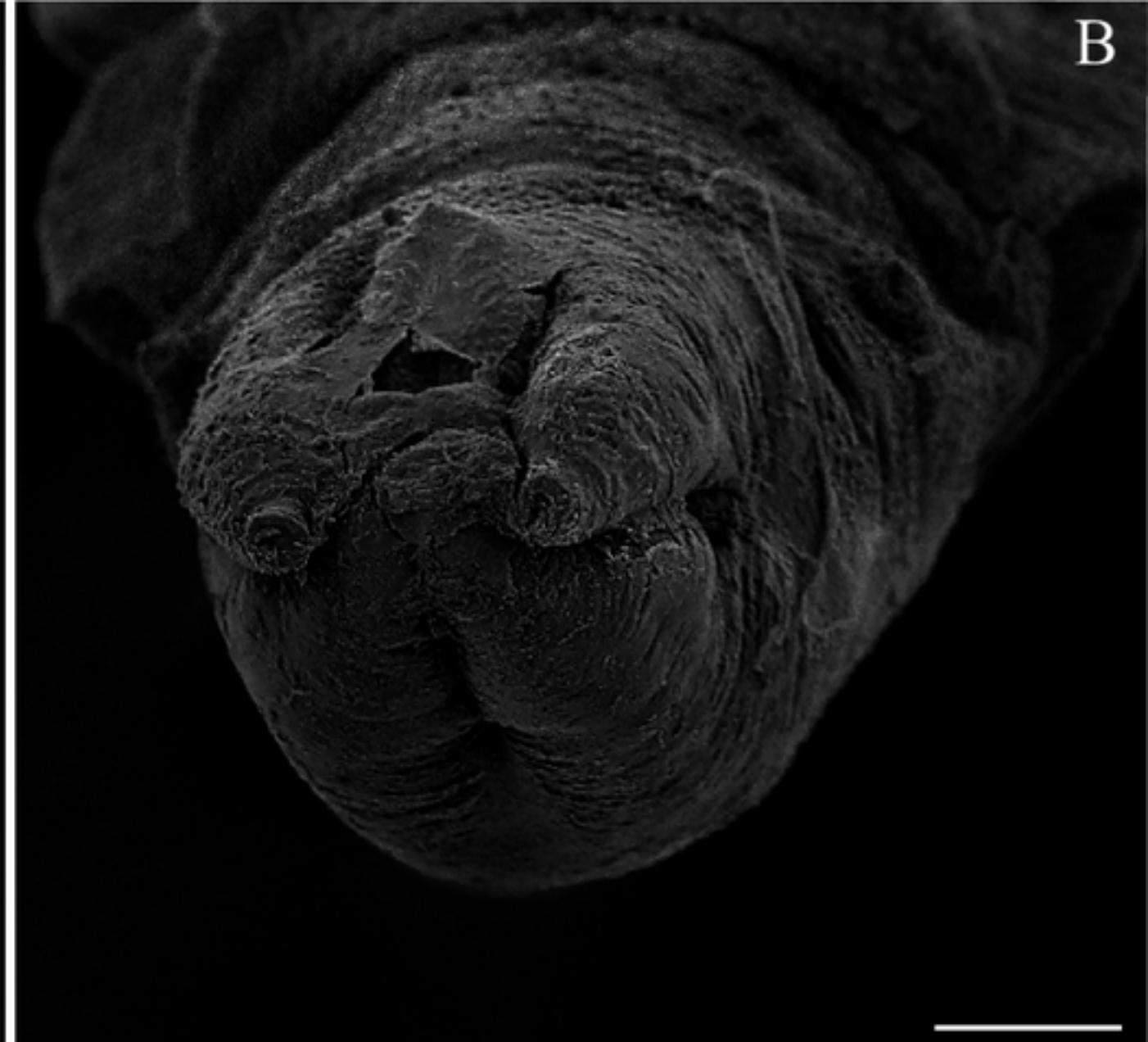


Figure 17